arXiv:1611.06207v1 [quant-ph] 18 Nov 2016

Time-of-arrival correlations

Charis Anastopoulos*and Nina Savvidou†
Department of Physics, University of Patras, 26500 Greece

November 21, 2016

Abstract

We propose that measurements of time-of-arrival correlations in multi-partite systems can sharply distinguish between different approaches to the time-of-arrival problem. To show this, we construct a Positive-Operator-Valued measure for two distinct time-of-arrival measurements in a bipartite system, and we prove that the resulting probabilities differ strongly from ones defined in terms of probability currents. We also prove that time-of-arrival correlations are entanglement witnesses, a result suggesting the use of temporal observables for quantum information processing tasks. Finally, we construct the probabilities for sequential time-of-arrival measurements on a single particle. We derive the state-reduction rule for time-of-arrival measurements; it differs significantly from the standard one, because time-of-arrival measurements are not defined at a single predetermined moment of time.

1 Introduction

The simplest version of the time-of-arrival problem in quantum mechanics [1, 2] is the following. A particle is prepared on an initial state $|\psi_0\rangle$ that is localized around $x = 0$ and has positive mean momentum. A detector is located at $x = L$. What is the probability $P(L, t)dt$ that the particle is detected at $x = L$ at some moment between t and $t + \delta t$?

In spite of the problem's apparent simplicity, there is no consensus on the answer. The reason is that there exists no self-adjoint operator for time in quantum mechanics [3]; hence, we cannot obtain an unambiguous answer by employing Born's rule. Several different approaches to the problem have been developed, each following a different reasoning. All approaches lead to probability densities $P(L, t)$ that differ from each other only at the level of small quantum fluctuations, so that they cannot easily be distinguished experimentally. Such a distinction would be highly desirable, because the time-of-arrival problem is only an elementary manifestation of an important foundational issue, namely, understanding the role of time in quantum mechanics.

*anastop@physics.upatras.gr
†ksavvidou@upatras.gr

The main idea of this paper is that different theories about the time-of-arrival could be distinguished if they are applied to more elaborate time-of-arrival measurements. Consider, for example, a multi-particle system. The time of arrival of each particle is a distinct observable that is recorded by different detectors. The correlations between different time-of-arrival observables are in principle measurable We expect that different theories will lead to different predictions for such correlations.

We implement this idea by extending the construction of time-of-arrival probabilities of Ref. [4] to set-ups that involve two or more time-of-arrival measurements. We express time-of-arrival correlations in terms of Positive-Operator-Valued Measures (POVMs). These correlations turn out to *differ significantly* from ones defined in terms of probability currents.

Our treatment of the time of arrival is based on the Quantum Temporal Probabilities (QTP) method [4, 5]. The QTP method provides an algorithm, applicable to any quantum system, that allows for the construction of quantum probabilities in which time is treated as a random variable. Besides the time-of-arrival problem [4, 6], the method has also been applied for the temporal characterization of tunneling [5, 7, 8], for calculating the response and correlations of accelerated particle detectors [9] and to relativistic quantum measurements [10]. The key idea is to distinguish between the time parameter of Schrödinger equation from the time of occurrence of a measurement event [11, 12]. The latter are physical observables: they are treated as quasiclassical macroscopic variables associated to a detector's degrees of freedom, and the associated probabilities are unambiguously defined [13].

The probability density with respect to the times of n particle detection events is a linear functional of a $2n$–correlation functions of the associated quantum field. The simplest time-of-arrival measurement involves one particle and one detector, hence, the detection probability is a linear functional of the two-point function [4]. The measurements considered in this paper involve two detection events; either one detection for each particle in a bi-partite system, or two successive detections of a single particle. The associated probability densities are linear functionals of field four-point functions.

Our analysis proceeds as follows. First, we revisit the time-of-arrival probability measure of Ref. [4]. We transform the measure to the classical state space, and study the properties of the quantum fluctuations. We find that different proposals about the time of arrival are distinguished at very low momenta (or equivalently, very low temperatures): the traversed distance must be of the order of the particles' thermal de Broglie wave-length.

Second, we consider time-of-arrival measurements in bipartite particle systems. We derive the joint probability distribution for the times of arrival t_1 and t_2 of the two particles. We prove that the resulting probabilities cannot, in general, be expressed in terms of probability currents. Thus, we prove that different approaches to the time of arrival lead to experimentally distinguishable predictions for time-of-arrival correlations. Moreover, we show that these correlation define *entanglement witnesses*. This result suggests that quantum temporal observables can be used for the detection of entanglement and, possibly, for information processing tasks.

Third, we consider sequential time-of-arrival measurements on a single particle. We derive the joint probability distribution for the times of arrival t_1 and t_2 at two spatially separated

detectors. We identify the rule for the change of the quantum state after a time-of-arrival measurement and show that it is very different from the usual 'state reduction' rule. We also define an observable for the time-of-flight velocity that differs, in general, from the canonical momentum observable.

The structure of this paper in the following. In Sec. 2, we set up our notation and present the time of arrival probabilities derived by the QTP method. In Sec. 3, we study the probabilities associated to a single time-of-arrival measurement. We focus on the properties of quantum fluctuations, and we discuss possible ways to distinguish experimentally between existing proposals. In Sec. 4, we consider time-of-arrival probabilities and correlations in composite systems. In Sec. 5, we consider sequential time-of-arrival measurements. In Sec. 6, we summarize and discuss our results.

2 Probability assignment

In this section, we set-up our notation and we present the time-of-arrival probabilities derived by the QTP method. The derivation is sketched in the Appendix A. For further details, see Refs. [10, 4, 5].

We consider a system of non-relativistic particles described by a Hilbert space $\mathcal{F}$. For identical particles, $\mathcal{F}$ a Fock space, either bosonic or fermionic. In the former case, $\mathcal{F}$ carries a representation of the canonical commutation relations

$$[\hat{a}_{\boldsymbol{k}}, \hat{a}_{\boldsymbol{k}'}] = [\hat{a}^\dagger_{\boldsymbol{k}}, \hat{a}^\dagger_{\boldsymbol{k}'}] = 0, \qquad [\hat{a}_{\boldsymbol{k}}, \hat{a}^\dagger_{\boldsymbol{k}'}] = \delta^3(\boldsymbol{k} - \boldsymbol{k}'), \tag{1}$$

expressed in terms of the bosonic annihilation and creation operators $\hat{a}_{\boldsymbol{k}}$ and $\hat{a}^\dagger_{\boldsymbol{k}}$.

In the latter case, $\mathcal{F}$ carries a representation of the canonical anti-commutation relations

$$\{\hat{c}_{\boldsymbol{k}}, \hat{c}_{\boldsymbol{k}'}\} = \{\hat{c}^\dagger_{\boldsymbol{k}}, \hat{c}^\dagger_{\boldsymbol{k}'}\} = 0, \qquad \{\hat{c}_{\boldsymbol{k}}, \hat{c}^\dagger_{\boldsymbol{k}'}\} = \delta^3(\boldsymbol{k} - \boldsymbol{k}'). \tag{2}$$

expressed in terms of the fermionic annihilation and creation operators $\hat{c}_{\boldsymbol{k}}$ and $\hat{c}^\dagger_{\boldsymbol{k}}$.

In what follows, we will ignore spin and internal degrees of freedom of the particles, as they do not affect time-of-arrival measurements. The quantum fields associated to the particles are

$$\hat{\psi}(\boldsymbol{x}) = \begin{cases} \int \frac{d^3k}{(2\pi)^{3/2}} e^{i\boldsymbol{k}\cdot\boldsymbol{x}} \hat{a}_{\boldsymbol{k}} & \text{for bosons} \\ \int \frac{d^3k}{(2\pi)^{3/2}} e^{i\boldsymbol{k}\cdot\boldsymbol{x}} \hat{c}_{\boldsymbol{k}} & \text{for fermions} \end{cases} \tag{3}$$

For bosons, the Hamiltonian on $\mathcal{F}$ is $\hat{h} = \int \frac{d^3k}{(2\pi)^3} \epsilon_{\boldsymbol{k}} \hat{a}^\dagger_{\boldsymbol{k}} \hat{a}_{\boldsymbol{k}}$ and for fermions $\hat{h} = \int \frac{d^3k}{(2\pi)^3} \epsilon_{\boldsymbol{k}} \hat{c}^\dagger_{\boldsymbol{k}} \hat{c}_{\boldsymbol{k}}$, where $\epsilon_{\boldsymbol{k}} = \frac{\boldsymbol{k}^2}{2m}$.

The QTP probability distribution for a particle to be detected at time t by a detector located at $\boldsymbol{L}$ is

$$P^{(1)}(\boldsymbol{L}, t) = C \int ds ds' \sqrt{f(t-s)f(t-s')} \langle \Psi_0 | Y^\dagger(\boldsymbol{L}, s') \hat{Y}(\boldsymbol{L}, s) | \Psi_0 \rangle,) \tag{4}$$

where C is a constant, and $|\Psi_0\rangle$ the initial state of the particle system.

The operator $\hat{Y}(\boldsymbol{x}, s)$ is the Heisenberg-picture evolution $e^{i\hat{h}s}\hat{Y}(\boldsymbol{x})e^{-i\hat{h}s}$ of a composite operator $\hat{Y}(\boldsymbol{x})$ that is a local functional of the quantum fields $\hat{\psi}(\boldsymbol{x})$. This operator originates from the interaction Hamiltonian between the particles and the detector. In what follows, we will consider two types of interaction,

1. $\hat{Y}(\boldsymbol{x}) = \hat{\psi}(\boldsymbol{x})$. This choice corresponds to a process in which the particle is absorbed during detection.

2. $\hat{Y}(\boldsymbol{x}) = \hat{\psi}^\dagger(\boldsymbol{x})\hat{\psi}(\boldsymbol{x})$. This choice corresponds to a process in which the particle is scattered during detection.

The smearing function f in Eq. (4) is centered around 0 with a width of order σ, the temporal coarse-graining of the detector. Smearing is essential for the definition of probabilities in the QTP method, because the time parameter t is a coarse-grained quasi-classical variable that coincides with the emergence of a macroscopic record of observation in the detector.

For example, we can employ Gaussian smearing functions

$$f(s) = \frac{1}{\sqrt{2\pi\sigma^2}} e^{-\frac{s^2}{2\sigma^2}}. \tag{5}$$

The Gaussians satisfy the useful identity

$$\sqrt{f(t-s)f_\sigma(t-s')} = f(t - \frac{s+s'}{2})g(s-s'), \tag{6}$$

where

$$g(s) = e^{-\frac{s^2}{8\sigma^2}}. \tag{7}$$

The analogue of Eq. (6) is also satisfied approximately for non Gaussian smearing functions. In such cases, g is a positive function that satisfies $g(0) = 1$ and $\lim_{|s|\to\infty} g(s) = 0$.

Using Eq. (6), the probability distribution $P(\boldsymbol{L}, t)$ can be expressed as a convolution

$$P^{(1)}(\boldsymbol{L}, t) = \int dt' f(t-t') P^{(1)}_{f.g.}(\boldsymbol{L}, t') \tag{8}$$

where

$$P^{(1)}_{f.g.}(\boldsymbol{L}, t) = C \int d\tau g(\tau) \langle \Psi_0 | Y^\dagger(\boldsymbol{L}, t - \frac{\tau}{2}) \hat{Y}(\boldsymbol{L}, t + \frac{\tau}{2}) | \Psi_0 \rangle, \tag{9}$$

is a probability distribution, finer than $P(\boldsymbol{L}, t)$, that usually takes a simple form.

The probability density associated to the measurement of one particle at time t_1 by a detector located at $\boldsymbol{L}_1$ and of on particle at time t_2 by a detector located at $\boldsymbol{L}_2$ is

$$P^{(2)}(\boldsymbol{L}_1,t_1;\boldsymbol{L}_2,t_2) = C\int ds_1 ds_1' ds_2 ds_2' \sqrt{f_1(t_1-s_1)f_1(t_1-s_1')f_2(t_2-s_2)f_2(t_2-s_2')} \\ \times\langle\Psi_0|\bar{\mathcal{T}}[\hat{Y}_1^\dagger(\boldsymbol{L}_1,s_1')\hat{Y}_2^\dagger(\boldsymbol{L}_2,s_2')]\mathcal{T}[\hat{Y}_2(\boldsymbol{L}_2,s_2)\hat{Y}_1(\boldsymbol{L}_1,s_1)]|\Psi_0\rangle, \quad (10)$$

where $\mathcal{T}$ stands for time-ordered product and $\bar{\mathcal{T}}$ for anti-time-ordered product. Eq. (10) takes into account the possibility that each detector may be associated to a different composite operator $\hat{Y}_i(\boldsymbol{x})$.

Again $P(\boldsymbol{L}_1,t_1;\boldsymbol{L}_2,t_2)$ can be expressed as a convolution

$$P^{(2)}(\boldsymbol{L}_1,t_1;\boldsymbol{L}_2,t_2) = \int dt_1' dt_2' f_1(t_1-t_1')f_2(t_2-t_2')P^{(2)}_{f.g.}(\boldsymbol{L}_1,t_1';\boldsymbol{L}_2,t_2'), \quad (11)$$

of a finer probability density

$$P^{(2)}_{f.g.}(\boldsymbol{L}_1,t_1;\boldsymbol{L}_2,t_2) = C\int d\tau_1 d\tau_2 g(\tau_1)g(\tau_2)\langle\Psi_0|\bar{\mathcal{T}}[\hat{Y}_1^\dagger(\boldsymbol{L}_1,t_1-\frac{\tau_1}{2})\hat{Y}_2^\dagger(\boldsymbol{L}_2,t_2-\frac{\tau_2}{2})] \\ \times\mathcal{T}[\hat{Y}_2(\boldsymbol{L}_2,t_2+\frac{\tau_2}{2})\hat{Y}_1(\boldsymbol{L}_1,t_1+\frac{\tau_1}{2})]|\Psi_0\rangle. \quad (12)$$

The probability densities (9) and (12) involve averaging over the temporal and not the spatial coordinates. They have been obtained using the approximation (111) in the Appendix A.2. Temporal averaging is essential for the definition of probabilities in the QTP method. This is not the case for spatial averaging. It is usually subsumed under the effects of temporal averaging and can be omitted for simplicity.

3 Single time-of-arrival measurement

In this section, we revisit the time-of-arrival probability derived in Ref. [4]. We examine its phase space properties, the classical limit, the associated uncertainties, and discuss how different candidates for the time-of-arrival probabilities might be distinguished experimentally.

3.1 The ideal probability distribution

We evaluate the fine-grained probability distribution (9) for a single detection of a particle of mass m. We consider the simplest case of particle detection by absorption, i.e., we choose $\hat{Y}(\boldsymbol{x}) = \hat{\psi}(\boldsymbol{x})$. The resulting probability distribution is the same for fermions and bosons

$$P^{(1)}_{f.g.}(\boldsymbol{L},t) = C\int \frac{d^3k d^3k'}{(2\pi)^3}\tilde{g}(\frac{\epsilon_{\boldsymbol{k}}+\epsilon_{\boldsymbol{k}'}}{2})e^{i(\boldsymbol{k}-\boldsymbol{k}')\cdot\boldsymbol{L}-i(\epsilon_{\boldsymbol{k}}-\epsilon_{\boldsymbol{k}'})t}\rho_0(\boldsymbol{k},\boldsymbol{k}'), \quad (13)$$

where $\tilde{g}$ is the Fourier transform of the function g. The function

$$\rho_0^{(1)}(\boldsymbol{k},\boldsymbol{k}') = \frac{1}{N}\langle\Psi_0|\hat{a}^\dagger_{\boldsymbol{k}'}\hat{a}_{\boldsymbol{k}}|\Psi_0\rangle \quad (14)$$

is the one-particle density matrix, where $|\Psi_0\rangle$ has been assumed a N-particle state. (In Eq. (13), a multiplicative factor of N has been absorbed in the constant C.)

Let the initial state be localized at $\boldsymbol{x} = 0$ and the detector at $\boldsymbol{x} = \boldsymbol{L}$. We reduce the system to one dimension along the axis that connects the particle source to the detector. The probability density (13) then becomes

$$P^{(1)}_{f.g.}(L,t) = C \int \frac{dkdk'}{2\pi} \tilde{g}(\frac{\epsilon_k + \epsilon_{k'}}{2}) e^{i(k-k')L - i(\epsilon_k - \epsilon_{k'})t} \rho^{(1)}_0(k,k'). \tag{15}$$

Eq. (15) is physically meaningful only for $t \geq 0$, but it can be mathematically extended to $t < 0$. For initial density matrices with support only on positive momenta k and localised at $x < L$, $P_{f.g.}(L,t)$ is strongly suppressed for negative t. Hence, when considering the total probability of detection $\mathrm{Prob}(L) := \int_0^\infty P_{f.g.}(L,t)$ we can extend the range of integration to the whole real axis. Then,

$$\mathrm{Prob}(L) = mC \int dk \frac{\tilde{g}(\epsilon_k)}{|k|} \rho^{(1)}_0(k,k). \tag{16}$$

The extension of integration to negative times is inadmissible for states with negative momentum, or for states with position support on both sides of the detector. Eq. (15) accounts also for these cases, but Eq. (16) does not apply.

We define the absorption rate $\alpha(\epsilon)$ of the detector as the fraction of particles with incoming energy ϵ that is absorbed by the detector. Eq. (16) implies that

$$\alpha(\epsilon) \sim \tilde{g}(\epsilon)/\sqrt{2m\epsilon}. \tag{17}$$

We choose the constant C, so that $\mathrm{Prob}(L)$ equals the fraction of detected particles. Then,

$$P^{(1)}_{f.g.}(L,t) = \int \frac{dkdk'}{2\pi} \alpha\left(\frac{\epsilon_k + \epsilon_{k'}}{2}\right) \sqrt{\frac{\epsilon_k + \epsilon_{k'}}{m}} e^{i(k-k')L - i(\epsilon_k - \epsilon_{k'})t} \rho^{(1)}_0(k,k'). \tag{18}$$

For a homogeneous detector of length $d << L$, the absorption rate is $\alpha(\epsilon) = \mu(\epsilon)d$, where $\mu(\epsilon)$ is the usual *attenuation coefficient* of the absorbing material. The attenuation coefficient can be measured directly, and it is a defining characteristic of the detector. In some cases, $\mu(\epsilon)$ can be computed from first principles as $n\sigma_{abs}$, where n is the number density of the individual absorbers and σ_{abs} is the absorption cross-section[1].

In what follows, we will consider *ideal detectors*, characterized by constant absorption rate. Normalizing so that $\mathrm{Prob}(L) = 1$, we obtain the *ideal* time-of-arrival probability distribution

$$P^{(1)}_{id}(L,t) = \int \frac{dkdk'}{2\pi} \sqrt{\frac{\epsilon_k + \epsilon_{k'}}{m}} e^{i(k-k')L - i(\epsilon_k - \epsilon_{k'})t} \rho^{(1)}_0(k,k'). \tag{19}$$

[1]The probability density $P^{(1)}_{f.g.}(L,t)$ of Eq. (18) is integrated with respect to all possible loci of detection, so it is not a density with respect to L. The corresponding density can be read immediately, by substituting the absorption rate $\alpha(\epsilon)$ with the attenuation coefficient $\mu(\epsilon)$.

For initial states with momentum spread much smaller than the mean momentum, we can approximate $\epsilon_k + \epsilon_{k'} = \frac{1}{2m}(k^2 + k'^2) = \frac{1}{2m}[(k-k')^2 + 2kk'] \simeq kk'/m$. Then, Eq. (19) coincides with the time-of-arrival probability distribution of Kijowski [14].

The probability density (19) is expressed as $Tr(\hat{\rho}\hat{\Pi}_L(t))$ where $\hat{\Pi}_L(t)$ are positive operators with matrix elements

$$\langle k|\hat{\Pi}_L(t)|k'\rangle = \frac{1}{2\pi}\sqrt{\frac{\epsilon_k + \epsilon_{k'}}{m}}e^{i(k-k')L - i(\epsilon_k - \epsilon_{k'})t}. \tag{20}$$

When restricted to the subspace of states with only positive values of momentum, and when all values $t \in \boldsymbol{R}$ are taken into account, $\hat{\Pi}_L(t)$ defines a POVM. For general initial states, we can define a POVM by including the positive operator associated to the event of no detection

$$\hat{\Pi}_L(\emptyset) = 1 - \int_0^\infty \hat{\Pi}(t)dt. \tag{21}$$

3.2 Time of arrival in the Wigner picture

We bring the ideal probability distribution (19) into a form that allows for a comparison with the classical time of arrival. To this end, we express the density matrix $\hat{\rho}_0^{(1)}$ in terms of its associated Wigner function

$$W_0(X,P) = \int \frac{dy}{2\pi}\langle X - \frac{y}{2}|\hat{\rho}_0^{(1)}|X + \frac{y}{2}\rangle e^{iPy}. \tag{22}$$

Substituting

$$\rho_0^{(1)}(k,k') = \frac{1}{2\pi}\int d\xi W_0(X, \frac{k+k'}{2})e^{-iX(k-k')}. \tag{23}$$

into Eq. (19), we obtain

$$P_{id}^{(1)}(L,t) = \int dXdP\frac{2P^2}{m}u[2P(L - X - \frac{t}{m}P)]W_0(X,P), \tag{24}$$

where

$$u(s) := \frac{1}{2\pi}\int_{-\infty}^{\infty} d\xi\sqrt{1+\xi^2}e^{i\xi s} = \frac{1}{\pi}\mathrm{Re}\int_0^\infty d\xi\sqrt{1+\xi^2}e^{i\xi s}. \tag{25}$$

The integral $u(s)$, Eq. (25) defines a distribution function that is singular at $s = 0$. The properties of the distribution u are analyzed in the Appendix B1.

For any $a > 0$,

$$u(as) = \frac{1}{2\pi a}\int_{-\infty}^{\infty} dy\sqrt{1+(y/a)^2}e^{iys}. \tag{26}$$

For large values of a, we can expand the square root, to obtain a formal series

$$u(as) = \frac{1}{a}\delta(s) - \frac{1}{2a^3}\delta''(s) - \frac{1}{8a^5}\delta''''(s) + \dots \tag{27}$$

We use Eq. (27) in order to express the probability density Eq. (24) as a series

$$P^{(1)}_{id}(L,t) = P^{(1)}_{cl}(L,t) + P^{(1)}_{1}(L,t) + P^{(2)}_{2}(L,t) + \dots \tag{28}$$

The first term in the series

$$\begin{aligned} P^{(1)}_{cl}(L,t) &= \int dX dP \frac{|P|}{m}\delta(L - X - \frac{P}{m}t)W_0(X,P) \\ &= \int dX dP \delta(t - m\frac{L-X}{P})W_0(X,P) \end{aligned} \tag{29}$$

coincides with the probability distribution associated to the *classical* time-of-arrival observable [15]

$$T_c(X,P) = \frac{m(L-X)}{P}. \tag{30}$$

The associated operator

$$\hat{T}_c = \frac{1}{2}[(L-\hat{x})\hat{p}^{-1} + \hat{p}^{-1}(L-\hat{x})] \tag{31}$$

was first studied by Aharonov and Bohm [16]. $\hat{T}_c$ is Hermitian but not self-adjoint. However, when restricted to states with support on positive momentum and well localised at positions $x < L$, $\hat{T}_c$ is indistinguishable from its self-adjoint variants [22, 23].

The action of $\hat{T}_c$ on states $|\psi\rangle$ with support on strictly positive momenta is well defined. For such states, $\hat{T}_c$ and the Hamiltonian $\hat{H}$ satisfy a canonical commutation relation.

$$[\hat{T}_c, \hat{H}]|\psi\rangle = -i|\psi\rangle. \tag{32}$$

The first correction to the classical distribution is

$$P^{(1)}_{1}(L,t) = -\frac{1}{8m}\int dP \frac{\partial^2_X W_0(L - \frac{P}{m}t, P)}{|P|}. \tag{33}$$

This term diverges, unless the Wigner function vanishes at $P = 0$.

3.3 Non-classical effects

The moment-generating function of the probability distribution (24) is

$$Z^{(1)}[\mu] := \int_{-\infty}^{\infty} dt P^{(1)}_{id}(t) e^{-i\mu t} = \langle e^{-i\mu T_c}\sqrt{1 + \frac{\mu^2}{16H^2}}\rangle \tag{34}$$

where $H(X,P) = \frac{P^2}{2m}$, and we wrote

$$\langle F \rangle = \int dX dP F(X,P) W_0(X,P) \tag{35}$$

in order to denote averaging with respect to the Wigner function W_0.

For $\langle \mu^2/H^2 \rangle << 1$, $Z^{(1)}[\mu]$ is well approximated by the generating function of the classical observable T_c. Thus, $P_{id}^{(1)}(L,t) \simeq P_{cl}^{(1)}(L,t)$, except for the regime of very low kinetic energies or very early times (large μ).

The expectation value $\bar{t}$ and the mean deviation Δt of the time of arrival are

$$\bar{t} = \langle T_c \rangle \tag{36}$$

$$(\Delta t)^2 = (\Delta T_c)^2 - \frac{1}{16}\langle H^{-2} \rangle. \tag{37}$$

For states with support on strictly positive momenta, Eq. (32) implies the uncertainty relation $\Delta T_c \Delta H \geq \frac{1}{4}$. Then, Eq. (37) becomes

$$(\Delta t)^2 \geq \frac{1}{4(\Delta H)^2} - \frac{1}{16}\langle H^{-2} \rangle. \tag{38}$$

The lower bound to Δt is smaller by what one would surmise from a naive application the Kennard-Robertson inequality to the time-of-arrival operator

The analogue of Eq. (38) for Kijowski's POVM has a plus sign in front of the $\langle H^{-2} \rangle$ term, and thus, implies that $(\Delta t) \geq \frac{1}{4}\sqrt{\langle H^{-2} \rangle}$. By Jensen's inequality, $\langle H^{-2} \rangle \geq \langle H \rangle^{-2}$, and an uncertainty relation $\langle H \rangle \Delta t \geq \frac{1}{4}$ follows. This is of the same form (modulo a constant of order unity) with the inequality derived in Ref. [17]. However, *no such uncertainty relation exists for the POVM (19).*

Two types of non-classical effects are manifested in the probability distribution Eq. (24). First, the classical time-of-arrival observable may exhibit quantum interference, as a consequence of the non-classical character of the initial state. In this case, the time of arrival behaves like any other phase space variable. An oscillating behavior of the Wigner function W_0 in some region of the phase space leads to interference terms in the probability distribution. For example, we consider a superposition state $c_1|\phi_1\rangle + c_2|\phi_2\rangle$, where $|\phi_1\rangle$ corresponds to a Wigner function localized at (X_1, P_1) and $|\phi_2\rangle$ corresponds to a Wigner function localized at (X_2, P_2). Then, the probability distribution for the time of arrival exhibits two peaks at $t_1 = T_{cl}(X_1, P_1)$ and $t_2 = T_{cl}(X_2, P_2)$ and by oscillatory terms in the intermediate values of t.

The other non-classical effect is that the time-of-arrival probability $P_{id}^{(1)}$ may differ significantly from the probability $P_{cl}^{(1)}$ that is defined in terms of the classical observable T_c. The difference between the two distributions is significant if $\Delta t \sqrt{\langle H^{-2} \rangle}$ is of order unity or smaller, and it is negligible if $\Delta t / \sqrt{\langle H^{-2} \rangle} >> 1$. The latter condition is satisfied if

$$\Delta t \langle H \rangle >> 1. \tag{39}$$

Eq. (39) is a classicality condition for the time of arrival [2].

[2] Conditions similar to Eq. (39) have appeared in several approaches to the time of arrival based upon

3.4 Distinguishing between different time-of-arrival proposals

While all physically reasonable proposals for the time-of-arrival probability have to coincide at the classical limit, they are expected to differ in their description of non-classical effects.

In order to avoid complications inessential to the main argument, we restrict to states with support on positive values of momentum, and localized at $x < L$, so that the probability of no detection is negligible. Hence, the probability density for the time of arrival is normalized to unity.

We will consider ideal probability distributions $P^{(1)}(L,t)$ that do not depend on any parameters that characterize the measuring apparatus. We assume that for large momenta, $P^{(1)}(L,t)$ the classical time-of-arrival variable T_c. These conditions imply that the moment-generating function $Z^{(1)}[\mu] := \int_{-\infty}^{\infty} dt P^{(1)}(L,t) e^{-i\mu t}$ has the form

$$Z^{(1)}[\mu] = \langle e^{-i\mu T_c} \eta(\mu/H) \rangle \tag{40}$$

for some positive function $\eta(x)$ of the dimensionless quantity $x = \mu/H$. The function η depends only on the ratio μ/H, because μ has the dimensions of energy, and in the absence of other parameters with dimension of energy (characterizing the apparatus), μ/H is the only possible combination.

We require that $\eta(x)$ satisfies the following properties.

(i) $\eta(0) = 1$, since $P^{(1)}(L,t)$ is normalized to unity.

(ii) $\eta'(0) = 0$, so that Eq. (36) holds. This condition guarantees that the expectation value always coincide with that of the classical observable T_c. Eq. (36) is the analogue of Ehrenfest's theorem for the time of arrival.

(iii) $\eta(-x) = \eta(x)$, so that the time-of-arrival probabilities are time-reversal covariant.

From Eq. (40), we express the probability density $P^{(1)}(L,t)$ in terms of the density matrix $\hat{\rho}^{(1)}$,

$$P^{(1)}(L,t) = \int \frac{dkdk'}{2\pi} \frac{k+k'}{2m} \eta\left(\frac{4(k'-k)}{k+k'}\right) e^{i(k-k')L - i(\epsilon_k - \epsilon_{k'})t} \rho_0^{(1)}(k,k'). \tag{41}$$

measurement models and/or complex potentials [18, 19, 20, 21]. In those models, Δt is not the mean deviation of the probability distribution, but the accuracy in the determination of the time of arrival. This quantity coincides with the temporal coarse-graining parameter σ that is introduced in the QTP method—see, Sec. 2. As a matter of fact, the first derivation of the probability density (19) required the hypothesis that $\sigma\langle H\rangle >> 1$ [6]. This condition was not necessary in later derivations that described the interaction between quantum particle and measurement apparatus in terms of local quantum fields [4].

The coarse-graining scale σ appears as a parameter in the absorption rate $\alpha(\epsilon)$ of the detector, and, as such, enters the probability distribution (18). The deviation from the ideal distribution (19) is σ-dependent; however, there is no *a priori* reason, why this dependence is stronger at the low momentum limit. In our opinion, the requirement that $\sigma\langle H\rangle >> 1$ is not a fundamental condition upon the measurability of the time of arrival.

The probability densities of the form (41) transform covariantly under time translations. They are special cases of Werner's time-of-arrival probability distribution [15].

Different choices of the function η correspond to different proposals for an ideal time-of-arrival probability distribution.

(i) The probability density (19) defined through the QTP method corresponds to $\eta(x) = \sqrt{1 + \frac{x^2}{16}}$.

(ii) Kijowski's probability distribution [14] corresponds to $\eta(x) = \sqrt{1 - \frac{x^2}{16}}$.

(iii) Several different proposals correspond to $\eta(x) = 1$. Proposals based on defining self-adjoint variants of the operator $\hat{T}_c$ [22, 23], lead to the probability density $P_{cl}^{(1)}(L,t)$ when restricted to states with positive momentum and $x < L$. This is also the case for the time-of-arrival probability defined by the probability current [1] and for some measurement models [24, 25].

All probability densities (41) have the same behavior at high momentum. This is also true for some proposed time-of-arrival probabilities that are non-covariant with respect to time translations [26]. Thus, the different proposals can only be distinguished by their predictions in the low momentum regime. However, moments such as $(\Delta T_c)^2$ and $\langle H^{-2}\rangle$ cannot be used for this purpose because they diverge.

We quantify the low momentum behavior of the time-of-arrival probabilities in terms of a temperature variable. We consider an initial state with a thermal distribution of positive momenta, at temperature β^{-1}

$$W_0(X,P) = n_0(X)\sqrt{\frac{2\beta}{\pi m}}e^{-\frac{1}{2}\beta P^2/m}\theta(P); \tag{42}$$

n_0 is a probability distribution for position with zero mean and mean deviation σ_X. For $\sigma_X << L$, we can substitute n_0 with a delta function. The probability density $P^{(1)}(L,t)$ turns out to be of the form $\int_0^\infty dx\eta(x)G(x)$, for some function $G(x)$. The exact form of $G(x)$ is not relevant, only the fact that $G(x)$ decays as $e^{-2mL^2x^2/\beta}$ for large x. If mL^2/β is significantly larger than unity, only values of x very close to zero contribute to the integral, and different functions $\eta(x)$ lead to the same probability density. Hence, a distinction between different candidate time-of-arrival probabilities is possible only if the quantity

$$\nu = \frac{\beta}{mL^2} \tag{43}$$

is at least of order one. This means that the *distance L between source and detector must be of the order of the thermal de Broglie wave-length of the particles.*

We also have to take into account that the temporal scale $\tau = L\sqrt{m\beta}$ for the measured time of arrival must be significantly larger than the time resolution of the apparatus. Lowering the temperature increases both ν and τ. For β^{-1} near a tenth of a milli-Kelvin, ν becomes

of order unity, while $\tau \sim 1\mu s$ is significantly larger than typical resolution of solid state detectors. Such a measurement requires $L \sim 30\mu m$ for electrons and $L \sim 1\mu m$ for neutrons.

These estimates suggest that the quantum regime above is not beyond present capabilities. Thus, an experimental distinction between different proposals for the time-of-arrival is possible in principle, even if the realization of such an experiment may very difficult. Perhaps, the distinction can be made easier in a different set-up, time-of-arrival measurements in multi-partite systems that are discussed in the following section.

4 Time of arrival in composite systems

The QTP method also applies to set-ups that involve more than one time-of-arrival measurement. In this section, we study time of arrival measurements in a bipartite system.

4.1 Probability assignment

We evaluate the fine grained probability distribution (12) for two detection events. We assume that both particles are absorbed at detection, i.e., $\hat{Y}_1(\boldsymbol{x}) = \hat{Y}_2(\boldsymbol{x}) = \hat{\psi}(\boldsymbol{x})$. Then,

$$P^{(2)}_{f.g.}(\boldsymbol{L}_1, t_1; \boldsymbol{L}_2, t_2) = C \int d^3k_1 d^3k_2 d^3k'_1 d^3k'_2 \tilde{g}(\frac{\epsilon_{\boldsymbol{k}_1} + \epsilon_{\boldsymbol{k}'_1}}{2}) \tilde{g}(\frac{\epsilon_{\boldsymbol{k}_2} + \epsilon_{\boldsymbol{k}'_2}}{2}) \\ \times e^{i(\boldsymbol{k}_1 - \boldsymbol{k}'_1)\cdot \boldsymbol{L}_1 - i(\epsilon_{\boldsymbol{k}_1} - \epsilon_{\boldsymbol{k}'_1})t_1} e^{i(\boldsymbol{k}_2 - \boldsymbol{k}'_2)\cdot \boldsymbol{L}_2 - i(\epsilon_{\boldsymbol{k}_2} - \epsilon_{\boldsymbol{k}'_2})t_2} \rho^{(2)}_0(\boldsymbol{k}_1, \boldsymbol{k}_2 | \boldsymbol{k}'_1, \boldsymbol{k}'_2), \tag{44}$$

where

$$\rho^{(2)}_0(\boldsymbol{k}_1, \boldsymbol{k}_2 | \boldsymbol{k}'_1, \boldsymbol{k}'_2) = \frac{1}{N^2 - N} \langle \Psi_0 | \hat{c}^\dagger_{\boldsymbol{k}'_1} \hat{c}^\dagger_{\boldsymbol{k}'_2} \hat{c}_{\boldsymbol{k}_2} \hat{c}_{\boldsymbol{k}_1} | \Psi_0 \rangle, \tag{45}$$

and $|\Psi_0\rangle$ was assumed to be a N-particle state. Eq. (44) applies for both bosons and fermions, the only difference being the symmetrization properties of the density matrix $\hat{\rho}^{(2)}_0$.

We consider a particle source localized at $\boldsymbol{x} = 0$ and two detectors localized at $\boldsymbol{x} = \boldsymbol{L}_1$ and $\boldsymbol{x}_2 = \boldsymbol{L}_2$, respectively. For distances $L_i = |\boldsymbol{L}_i|$ much larger than the dimensions of the source, we can treat each particle as one dimensional, moving along the axis connecting the source to the detector. Following the procedure of Sec. 3.1, we obtain an ideal probability distribution that generalizes Eq. (19),

$$P^{(2)}_{id}(L_1, t_1; L_2, t_2) = \int \frac{dk_1 dk'_1 dk_2 dk'_2}{4\pi^2 m^2} \sqrt{\frac{\epsilon_{k_1} + \epsilon_{k'_1}}{m}} \sqrt{\frac{\epsilon_{k_2} + \epsilon_{k'_2}}{m}} \\ \times e^{i(k_1 - k'_1)L_1 - i(\epsilon_{k_1} - \epsilon_{k'_1})t_1} e^{i(k_2 - k'_2)L_2 - i(\epsilon_{k_2} - \epsilon_{k'_2})t_2} \rho^{(2)}_0(k_1, k_2; , k'_1, k'_2) \tag{46}$$

Eq. (46) can be written as

$$P^{(2)}_{id}(L_1, t_1; L_2, t_2) = Tr\left[\hat{\rho}^{(2)}_0 \hat{\Pi}_{L_1}(t_1) \otimes \hat{\Pi}_{L_2}(t_2)\right], \tag{47}$$

where the positive operators $\hat{\Pi}_L(t)$ are given by Eq. (20).

It is straightforward to express the probability density (47) in terms of a Wigner function $W_0(X_1, X_2, P_1, P_2)$ for a pair of particles

$$P_{id}^{(2)}(L_1, t_1; L_2, t_2) = \int d^2X d^2P \frac{4P_1^2 P_2^2}{m^2} u[2P_1(L_1 - X_1 - \frac{t_1}{m}P_1)] \times u[2P_2(L_2 - X_2 - \frac{t_2}{m}P_2)] W_0(X_1, X_2, P_1, P_2). \quad (48)$$

The corresponding moment-generating function is

$$Z^{(2)}[\mu_1, \mu_2] := \int dt_1 dt_2 P_{id}^{(2)}(L_1, t_1; L_2, t_2) e^{-i\mu_1 t_1 - i\mu_2 t_2} = \langle e^{-i\mu_1 T_{c1} - i\mu_2 T_{c2}} \sqrt{1 + \frac{\mu_1^2}{16H_1^2}} \sqrt{1 + \frac{\mu_2^2}{16H_2^2}} \rangle. \quad (49)$$

The probability density (47) has to be supplemented with probabilities for the events of no detection in either detector, namely,

$$P_{id}^{(2)}(L_1, \emptyset; L_2, t_2) = Tr\left[\hat{\rho}_0 \hat{\Pi}_{L_1}(\emptyset) \otimes \hat{\Pi}_{L_2}(t_2)\right] \quad (50)$$

$$P_{id}^{(2)}(L_1, t_1; L_2, \emptyset) = Tr\left[\hat{\rho}_0 \hat{\Pi}_{L_1}(t_1) \otimes \hat{\Pi}_{L_2}(\emptyset)\right], \quad (51)$$

$$\mathrm{Prob}_{id}^{(2)}(L_1, \emptyset; L_2, \emptyset) = Tr\left[\hat{\rho}_0 \hat{\Pi}_{L_1}(\emptyset) \otimes \hat{\Pi}_{L_2}(\emptyset)\right]. \quad (52)$$

Using Eq. (21) we obtain a relation between $P^{(2)}$ and $P^{(1)}$

$$\int_0^\infty dt_2 P_{id}^{(2)}(L_1, t_1; L_2, t_2) + P_{id}^{(2)}(L_1, t_1; L_2, \emptyset) = P^{(1)}(L_1, t_1). \quad (53)$$

As in Sec. 3.1, the probabilities (50—52) vanish for initial states with support only on positive values of momenta. In this case,

$$\int_0^\infty dt_2 P_{id}^{(2)}(L_1, t_1; L_2, t_2) = P^{(1)}(L_1, t_1). \quad (54)$$

Eq. (47) also applies for pairs of distinguishable particles. The derivation requires the use of a different field for each type of particle, otherwise, it proceeds in exactly the same way. The differences are that (i) the initial density matrix $\hat{\rho}_0^{(2)}$ is not restricted to the antisymmetric or symmetric subspace of the particle's Hilbert space and (ii) that the two particles may have different masses.

4.2 Incompatibility with probability currents

The use of probability currents is the oldest, and arguably the simplest, approach to the time-of-arrival problem. The time-of-arrival probability density for a single particle is the

expectation value of a current operator $\hat{J}(L,t)$ as $\langle\psi_0|\hat{J}(L,t)|\psi_0\rangle$ on an initial state $|\psi_0\rangle$. The usual probability current of Schrödinger's equation corresponds to

$$\hat{J}(L,t) = e^{i\hat{H}t}[\hat{p}\delta(\hat{x}-L) + \delta(\hat{x}-L)\hat{p}]e^{-i\hat{H}t}. \tag{55}$$

This choice for $\hat{J}(L,t)$ is not satisfactory, because it does not lead to positive definite probabilities [27, 28]. However, the probability densities obtained from POVMs can be expressed as operator-ordered variations of the Schrödinger current. For example, Kijowski's probabilities correspond to a current operator

$$\hat{J}(L,t) = e^{i\hat{H}t}|\hat{p}|^{1/2}\delta(\hat{x}-L)|\hat{p}|^{1/2}e^{-i\hat{H}t}. \tag{56}$$

Thus, for a single particle, approaches based on the notion of a probability current do not lead to significantly different predictions from the time-of-arrival POVMs. This equivalence fails in multi-partite systems. Time-of-arrival probabilities defined in terms of probability currents should be of the form

$$P^{(1)}(L,t) = \langle\Psi_0|\hat{J}(L,t)|\Psi_0\rangle \tag{57}$$

$$P^{(2)}(L_1,t_1;L_2,t_2) = \langle\Psi_0|\hat{J}(L_1,t_1)\hat{J}(L_2,t_2)|\Psi_0\rangle, \tag{58}$$

for $|\Psi_0\rangle \in \mathcal{F}$ some current operator $\hat{J}(L,t)$ on $\mathcal{F}$. The current operator should satisfy $[\hat{J}(L_1,t_1),\hat{J}(L_2,t_2)] = 0$, so that the probability (58) is real-valued.

For systems of identical particles, Eqs. (57—58) are not compatible with Eqs. (19) and (52). To see this, consider a two-particle state $|\Psi_0\rangle$. Comparing Eq. (57) with Eq. (58) we find that

$$\hat{J}(L_1,t_1) = \frac{1}{2}\left(\hat{\Pi}_L(t)\otimes\hat{1} + \hat{1}\otimes\hat{\Pi}_L(t)\right), \tag{59}$$

where we have taken into account that any physical operator must be invariant under exchange of the two identical particles. Comparing Eq. (58) and Eq. (52), we obtain

$$\hat{J}(L_1,t_1)\hat{J}(L_2,t_2) = \hat{\Pi}_{L_1}(t_1)\otimes\hat{\Pi}_{L_2}(t_2) \tag{60}$$

Eqs. (59) and (60) are clearly incompatible. The time-of-arrival probabilities obtained by the QTP method cannot be expressed in terms of a probability current. In fact, any approach to the time-of-arrival in terms of POVMs would lead to an Eq. similar to (47) when applied to composite systems. We conclude that *current-based approaches strongly disagree with POVM-based approaches* in multi-partite systems.

Probabilities defined in terms of a current operator are subject to constraints that do not apply to probabilities defined through POVMs. To prove this, we first define the two-time *coherence function*

$$C^{(2)}(L_1,t_1;L_2,t_2) = \frac{P^{(2)}(L_2,t_2;L_1,t_1)}{P^{(1)}(L_1,t_1)P^{(1)}(L_2,t_2)}, \tag{61}$$

where the probability distributions $P^{(2)}(L_2, t_2; L_1, t_1)$ and $P^{(1)}(L, t)$ satisfy Eq. (54).

The diagonal elements of $C^{(2)}$ define the *coincidence function*,

$$c^{(2)}(L, t) := C^{(2)}(L, t; L, t) \tag{62}$$

For $c^{(2)}(L, t) > 1$ simultaneous detection is more probable than what would be predicted if the events were statistical independent, while for $c^{(2)}(L, t) < 1$ simultaneous detection is less probable.

For the probability densities (57—58), the coincidence function satisfies

$$c^{(2)}(L, t) = \frac{\langle \hat{J}(L, t)^2 \rangle}{\langle \hat{J}(L, t) \rangle^2} \geq 1 + \left(\frac{\Delta J(L, t)}{\langle \hat{J}(L, t) \rangle} \right)^2 \geq 1, \tag{63}$$

where $\Delta J(L, t)$ stands for the standard deviation of $\hat{J}(L, t)$. Thus, any measurement of the coincidence function that violates Eq. (63) for some value of t disproves the definition of time-of-arrival probabilities in terms of probability currents.

In Sec. 4.4, we present explicit examples of coincidence functions violate Eq. (63) very strongly. For example, for some fermionic quantum states, $c^{(2)}(L, t)$ may vanish. These examples strongly suggest that the violation of (63) is measurable, and so is the distinction between POVM-based and current-based approaches to the time-of-arrival problem.

4.3 Non-classical correlations

Consider a bipartite particle system described by a *classical* probability density $\rho_0(\xi)$ on a state space Γ. The joint probability for two time-of-arrival measurements is of the form

$$P^{(2)}(L_1, t_1; L_2, t_2) = \int d\xi \rho_0(\xi) F_{L_1, t_1}(\xi) F_{L_2, t_2}(\xi), \tag{64}$$

where $F_{L,t}$ are positive valued functions on Γ. The classical probability density (64) is subject to constraints that do not limit the quantum probability density (48). We shall express some of these constraints in terms of two inequalities for the coherence function (61).

The first constraint follows from the Cauchy-Schwartz inequality for Eq. (58),

$$P^{(2)}(L_2, t_2; L_1, t_1) \leq \sqrt{P^{(2)}(L_2, t_2; L_2, t_2) P^{(2)}(L_1, t_1; L_1, t_1)}, \tag{65}$$

or equivalently,

$$C^{(2)}(L_1, t_1; L_2, t_2) \leq \sqrt{c^{(2)}(L_1, t_1) c^{(2)}(L_2, t_2)}. \tag{66}$$

We shall refer to Eq. (66) as the *C-S constraint*.

The second constraint is formally identical with Eq. (63),

$$c^{(2)}(L, t) = \frac{\langle F_{L,t}^2 \rangle}{\langle F_{L,t} \rangle^2} \geq 1, \tag{67}$$

where here $\langle \ldots \rangle$ stands for averaging with respect to ρ_0.

We shall refer to Eq. (63) as the *bunching* condition, meaning that the simultaneous detection of particles is enhanced. The condition $c^{(2)}(L,t) < 1$ will be referred to as *antibunching*[3]. Both constraints can be violated by systems prepared in an entangled state—some examples are provided in Sec. 4.4. Therefore, *time-of-arrival measurements define entanglement witnesses*. The relation between time of arrival, entanglement and other quantum resources will be elaborated in other publications.

Here we restrict to a simple example that demonstrates how entanglement information is encoded into time-of-arrival correlations. For simplicity, we will consider a system of distinguishable particles, in order to avoid subtleties in the definition of separability in systems of identical particles. We characterize separability using the Peres-Horodecki criterion [30] for continuous variables [31].

We restrict to states $\hat{\rho}_0^{(2)}$ with strictly positive momentum content for both particles, so that the action of the operators $\hat{T}_{ci}$ is well defined. Then we define the operators $\hat{T}_\pm = \hat{T}_{c1} \pm \hat{T}_{c2}$ and $\hat{H}_\pm = \hat{H}_1 \pm \hat{H}_2$. For any separable state, the following inequalities hold

$$\Delta H_+ \Delta T_- \geq 1 \qquad \Delta H_- \Delta T_+ \geq 1. \tag{68}$$

We evaluate the mean deviation of the variables, $t_\pm = t_1 \pm t_2$ with respect to the probability distribution (48)

$$(\Delta t_\pm)^2 = (\Delta T_\pm)^2 - \frac{1}{16}\langle H_1^{-2} + H_2^{-2} \rangle. \tag{69}$$

Thus, for a separable initial state, the following inequalities are satisfied

$$(\Delta t_\pm)^2 \geq \frac{1}{(\Delta H \mp)^2} - \frac{1}{16}\langle H_1^{-2} + H_2^{-2} \rangle. \tag{70}$$

Conversely, if Eq. (70) is violated, the state of the system is entangled.

We specialize to the case of an initial density matrix that is symmetric under particle exchange. Then, $(\Delta t_1)^2 = (\Delta t_2)^2 = (\Delta t)^2$, $(\Delta H_1)^2 = (\Delta H_2)^2 = (\Delta H)^2$, and $\langle H_1^2 \rangle = \langle H_2^2 \rangle = \langle H^2 \rangle$. For this state, $(\Delta t_\pm)^2 = 2(\Delta t)^2 \pm 2C_{t_1 t_2}$ and $(\Delta H_\pm)^2 = 2(\Delta H)^2 \pm 2C_{H_1 H_2}$, where $C_{AB} = \langle AB \rangle - \langle A \rangle \langle B \rangle$ is the correlation function of the observables A and B. Then, the separability conditions (70) become

$$(\Delta t)^2 \pm C_{t_1 t_2} \geq \frac{1}{4((\Delta H)^2 \mp C_{H_1 H_2})} - \frac{1}{16}\langle H^{-2} \rangle. \tag{71}$$

[3]We decided to use a different terminology from quantum optics, where bunching refers to the analogue of Eq. (66) (for stationary or almost stationary states) and condition (63) is referred to as "super-Poissonian photon statistics" [29]. Unlike photons, massive particles do not exhibit superpositions of different particle number. Hence, notions related to the distribution of particle numbers are not useful.

4.4 An example

We evaluate the probability density (47) for states of the form

$$|\Psi_0\rangle = \frac{1}{\sqrt{2}}\left(|\psi_1\rangle \otimes |\psi_2\rangle \pm |\psi_2\rangle \otimes |\psi_1\rangle\right), \tag{72}$$

for two orthogonal single-particle states $|\psi_1\rangle$ and $|\psi_2\rangle$. The plus sign in Eq. (72) corresponds to bosonic and the minus sign to fermionic particles.

We assume that $|\psi_1\rangle$ has support at large momenta, so that the corresponding single-time probability densities (41) are indistinguishable; we assume the same for $|\psi_2\rangle$. Then we can approximate $\hat{\Pi}_L(t)$ with Kijowski's POVM, so that $\langle\psi_j|\hat{\Pi}_L(t)|\psi_i\rangle = a_i(L,t)a_j^*(L,t)$, where

$$a_i(L,t) = \int \frac{dk}{\sqrt{2\pi}}\sqrt{|k|}e^{ikL - i\epsilon_k t}\tilde{\psi}_i(k). \tag{73}$$

Then, we obtain

$$P_{id}^{(1)}(L,t) = \frac{1}{2}\left[|a_1(L_1,t_1)|^2 + |a_2(L_2,t_2)|^2\right] \tag{74}$$

$$\begin{aligned} P_{id}^{(2)}(L_1,t_1;L_2,t_2) &= \frac{1}{2}\left[|a_1(L_1,t_1)a_2(L_2,t_2)|^2 + |a_1(L_2,t_2)a_2(L_1,t_1)|^2\right. \\ &\pm \left. 2\mathrm{Re}\left(a_1(L_1,t_1)a_2^*(L_1,t_1)a_2(L_2,t_2)a_1^*(L_2,t_2)\right)\right], \end{aligned} \tag{75}$$

The coincidence function $c^{(2)}(L,t)$ vanishes identically for fermions. Eq. (67) is thus violated: fermions exhibit anti-bunching behavior at all times.

For bosons,

$$c^{(2)}(L,t) = 1 - \frac{[|a_1(L,t)|^2 - |a_2(L,t)|^2]^2 - 4|a_1(L,t)a_2(L,t)|^2}{[|a_1(L,t)|^2 + |a_2(L,t)|^2]^2} \tag{76}$$

Plots of $c^{(2)}(L,t)$ are given in Fig. 1 for a specific choice of initial states. Bosons exhibit either bunching or anti-bunching behavior at different times. Fig. 1 also demonstrates that the coincidence function contains information that is not accessible from single time-of-arrival measurements.

The C-S constraint (66) is always violated for fermions, since $c^{(2)}(L,t) = 0$ even when the coherence function $C^{(2)}(L_1,t_1;L_2,t_2)$ is non zero. In Fig.2, we plot $C^{(2)}(L_1,t_1;L_2,t_2)$ for a specific choice of initial state. The coherence function is characterized by oscillations, with a characteristic frequency of the order of $|\bar{E}_1 - \bar{E}_2|$, where $\bar{E}_i$ is the mean energy of the state $|\psi_i\rangle$. Whether such oscillations are observable or not depends on the scale σ of temporal coarse-graining. The probability density (46) is a special case of the probability density (12). This implies that smearing at a scale of σ is required in order to obtain the observable probabilities (11. Hence, the oscillations of $C^{(2)}(L_1,t_1;L_2,t_2)$ are observable only if $|\bar{E}_1 - \bar{E}_2|\sigma$ is at most of order unity.

For bosons, we evaluate the ratio

$$h(t_1,t_2) = \frac{\sqrt{c^{(2)}(L,t_1)c^{(2)}(L,t_2)}}{C^{(2)}(L_1,t_1;L_2,t_2)}, \tag{77}$$

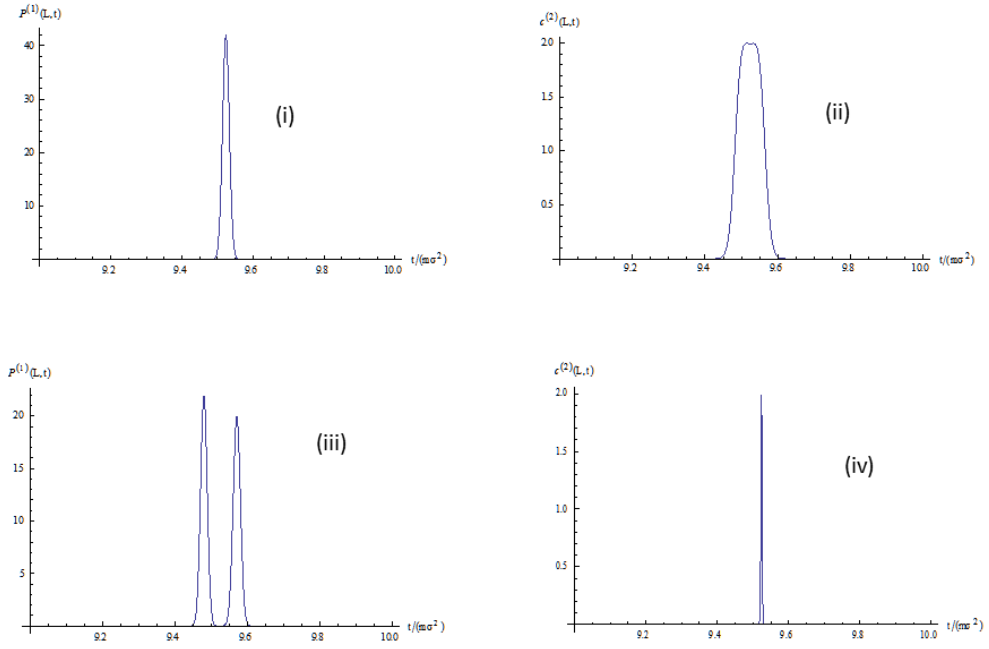

Figure 1: Single-time probability densities and coincidence functions for an initial state of the type (72), where $\psi_i(x) = \phi(x - x_i)e^{ip_i x}$, for some constants $x_i, p_i, i = 1, 2$. We choose for $\phi(x)$ a Gaussian $\phi(x) = (2\pi\sigma_x^2)^{-1/4} exp[-x^2/(4\sigma_X^2)]$. For $|x_2 - x_1| >> \sigma_X$, ψ_1 and ψ_2 are orthogonal. The mean time of arrival for each wave-packet is $\bar{t}_i = m(L - x_i)/p_i$. We have chosen $L/\sigma_X = 1000, p_1\sigma_X = 100, p_2\sigma_X = 110$. In plots (i) and (ii), $\bar{t}_1 = \bar{t}_2$. The superposition cannot be identified at the level of the probability density $P_{id}^{(1)}(L, t)$ of Plot (i). Plot (ii) describes the coincidence function $c^{(2)}(L, t)$ as a function of $t/(m\sigma_X^2)$ for bosons. Bunching or anti-bunching behavior is time-dependent. Plots (iii) and (iv) are the same as (i) and (ii) only with $\bar{t}_1 = 0.9\bar{t}_2$. There are two distinguishable peaks in the probability density, and the peak in $c^{(2)}(L, t)$ is sharper.

which is larger than unity when the C-S constraint is satisfied. In Fig. 3, $h(t_1, t_2)$ is evaluated for a specific initial state. It takes values both larger and smaller than unity, so the C-S constraint is violated also for bosons.

5 Sequential time-of-arrival measurements

In this section, we consider two successive time-of-arrival measurements on the same particle. We find how the quantum state changes after a time-of-arrival measurement and we construct the probabilities for the time-of-flight velocity.

5.1 Probability assignment

Two successive measurements can be performed on a single particle only if the first measurement does not annihilate the particle. In the QTP method, this implies that the com-

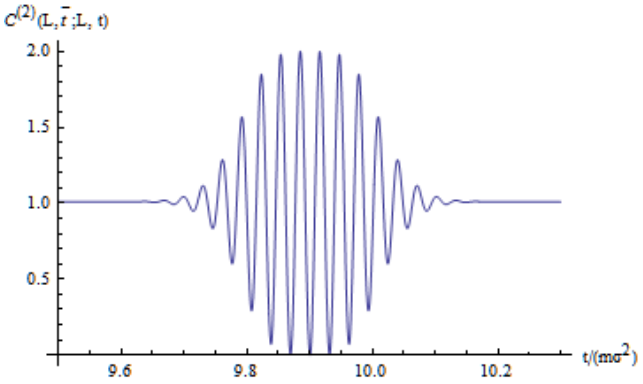

Figure 2: Coherence function $C^{(2)}(L, t_1; L, t_2)$ for an initial fermionic state of the type (72), where $\psi_i(x) = \phi(x - x_i)e^{-p_i x}$, for some constants $x_i, p_i, i = 1, 2$; $\phi(x)$ is the same Gaussian as in Fig. 1. We have chosen $L/\sigma_X = 1000, p_1\sigma_X = 100, p_2\sigma_X = 102$, and x_i so that the mean times of arrival of each wave-packet have the same value $\bar{t}$. In the plot, we fix $t_1 = \bar{t}$, and vary t_2 using dimensionless units.

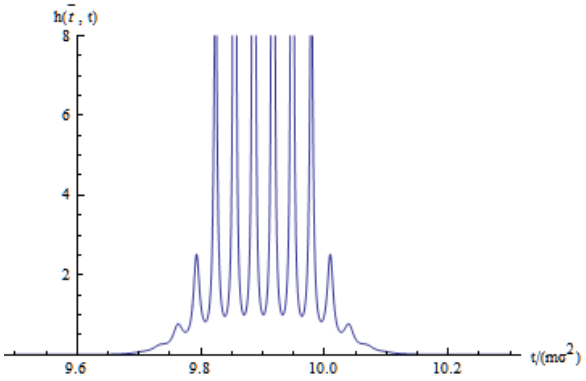

Figure 3: The ratio $h(t_1, t_2)$,Eq. (77), evaluated for a bosonic initial state of the form (72), for the same $\psi_i(x)$ with Fig. 2. Both wave packets $\psi_i(x)$ have the same mean time of arrival $\bar{t}$. In the plot, we fix $t_1 = \bar{t}$, and vary t_2 using dimensionless units.

posite operator $\hat{Y}_1(\boldsymbol{x})$ of Eq. (10) must describe particle scattering rather than absorption, i.e., $\hat{Y}_1(\boldsymbol{x}) = \hat{\psi}^\dagger(\boldsymbol{x})\hat{\psi}(\boldsymbol{x})$. There is no constraint for the second measurement, so we take $\hat{Y}_2(\boldsymbol{x}) = \hat{\psi}(\boldsymbol{x})$, as in Secs. 3 and 4.

Eq. (10) for an one-particle initial state $|\Psi_0\rangle = \int d^3k \psi_0(\boldsymbol{k})\hat{a}^\dagger_{\boldsymbol{k}}|0\rangle$ yields

$$P^{(2)}_{f.g}(\boldsymbol{L}_1, t_1; \boldsymbol{L}_2, t_2) = C \int \frac{d^3k_1 d^3k_2 d^3k'_1 d^3k'_2}{(2\pi)^9}\, \tilde{g}_1\left(\frac{\epsilon_{\boldsymbol{k}_1} - \epsilon_{\boldsymbol{k}_2} + \epsilon_{\boldsymbol{k}'_1} - \epsilon_{\boldsymbol{k}'_2}}{2}\right) \tilde{g}_2\left(\frac{\epsilon_{\boldsymbol{k}_2} + \epsilon_{\boldsymbol{k}'_2}}{2}\right)$$
$$\times e^{i(\boldsymbol{k}_2 - \boldsymbol{k}'_2)\cdot \boldsymbol{L}_2 - i(\epsilon_{\boldsymbol{k}_2} - \epsilon'_{\boldsymbol{k}_2})t_2} e^{i(\boldsymbol{k}_1 - \boldsymbol{k}_2 - \boldsymbol{k}'_1 + \boldsymbol{k}'_2)\cdot \boldsymbol{L}_1 - i(\epsilon_{\boldsymbol{k}_1} - \epsilon_{\boldsymbol{k}_2} - \epsilon_{\boldsymbol{k}'_1} + \epsilon_{\boldsymbol{k}'_2})t_1} \tilde{\psi}_0(\boldsymbol{k}'_1)\tilde{\psi}_0(\boldsymbol{k}_1). \quad (78)$$

where $\tilde{g}_i$ are the Fourier transforms of the functions g_i.

In general, the particle can scatter towards any direction after the first measurement. We restrict to propagation along the axis connecting the source to the locus $\boldsymbol{L}_1$ of the first detector, and then along the axis $\boldsymbol{L}_2 - \boldsymbol{L}_1$ connecting the loci of the two apparatuses. The assumption that $\boldsymbol{L}_1$ and $\boldsymbol{L}_2$ are parallel incurs no loss of generality and allows us to use a notation for an one-dimensional problem.

For an initial state with positive momentum, Eq. (78) becomes

$$P^{(2)}_{f.g}(L_1, t_1; L_2, t_2) = C \int \frac{dk_1 dk_2 dk'_1 dk'_2}{(2\pi)^3}\, \tilde{g}_1\left(\frac{\epsilon_{k_1} - \epsilon_{k_2} + \epsilon_{k'_1} - \epsilon_{k'_2}}{2}\right) \tilde{g}_2\left(\frac{\epsilon_{k_2} + \epsilon_{k'_2}}{2}\right)$$
$$\times \theta(k_2)\theta(k'_2) e^{i(k_2 - k'_2)\cdot L_2 - i(\epsilon_{k_2} - \epsilon_{k'_2})t_2}\, e^{i(k_1 - k_2 - k'_1 + k'_2)L_1 - i(\epsilon_{k_1} - \epsilon_{k_2} - \epsilon_{k'_1} + \epsilon_{k'_2})t_1} \tilde{\psi}^*_0(k'_1)\tilde{\psi}_0(k_1). \quad (79)$$

We have restricted the integration to positive values of k_2 and k'_2, since particles exiting the first detector with negative momenta with negative momenta will not be recorded by the second detector[4].

The probability densities (79) are strongly suppressed, if $t_1 < 0$ or if $t_2 < t_1$. Hence, the total probability $\mathrm{Prob}(L_1, L_2)$ that two detection events have occurred is well approximated by integrating $P^{(2)}_{f.g}$ along the whole real axis for both t_1 and t_2. Then,

$$\mathrm{Prob}(L_1, L_2) := \int_{-\infty}^{\infty} dt_1 \int_{-\infty}^{\infty} dt_2 P^{(2)}_{f.g}(L_1, t_1; L_2, t_2)$$
$$= Cm^2 \int \frac{dk_1 dk_2}{2\pi|k_1 k_2|} \tilde{g}_1(\epsilon_{k_1} - \epsilon_{k_2})\tilde{g}_2(\epsilon_{k_2})\theta(k_2)|\tilde{\psi}_0(k_1)|^2. \quad (80)$$

Eq. (80) implies that

(i) $\tilde{g}_2(\epsilon_k)/|k|$ is the absorption coefficient of the second detector, and

(ii) $\frac{1}{|k_1|}\tilde{g}_1(\epsilon_{k_1} - \epsilon_{k_2})$ is the probability that an incoming particle of momentum k_1 is scattered to a different momentum k_2.

[4]The positivity of k_2 and k'_2 is not an additional assumption. We phrased it as such because in this paper we ignore position coarse-graining—we employ the approximation (111) in the Appendix A.2. Suppose we smear Eq. (79) with respect to the position L_1. If the smearing length is sufficiently large, a delta function $\delta(k_1 - k_2 - k'_1 + k'_2)$ appears. Together with the constraints to the energies from $\tilde{g}_1$, it guarantees the positivity of k_2 and k'_2. The particle does not back-scatter as a result of the first time-of-arrival measurement.

We consider ideal detectors. For the first detector, the idealization consists in the assumption that energy transfer during scattering is negligible. For the second detector, the idealization is the same with Sec. 3.1., i.e., we assume that particle absorption in the second detector is independent of the particle's momentum. These conditions imply that $\tilde{g}_1(\epsilon_k - \epsilon_{k'}) \sim \epsilon_k \delta(\epsilon_k - \epsilon_{k'})$ and that $g_2(\epsilon) \sim \sqrt{\epsilon}$. Choosing the constant C so that $\mathrm{Prob}(L_1, L_2) = 1$, we obtain the ideal probability distribution

$$P^{(2)}_{id}(L_1, t_1; L_2, t_2) = \int \frac{dk_1 dk_2 dk'_1 dk'_2}{2\pi^2} \left(\frac{\epsilon_{k_1} + \epsilon_{k'_1}}{m} \right)^{3/2} \delta(\epsilon_{k_1} - \epsilon_{k_2} + \epsilon_{k'_1} - \epsilon_{k'_2}) \theta(k_2) \theta(k'_2) \times e^{i(k_2 - k'_2)\cdot L_2 - i(\epsilon_{k_2} - \epsilon_{k'_2})t_2} \, e^{i(k_1 - k_2 - k'_1 + k'_2)L_1 - i(\epsilon_{k_1} - \epsilon_{k_2} - \epsilon_{k'_1} + \epsilon_{k'_2})t_1} \tilde{\psi}^*_0(k'_1) \tilde{\psi}_0(k_1). \quad (81)$$

Eq. (81) does not have the standard form of probability densities for sequential measurements. If the observable A corresponding to a POVM $\hat{E}(a)$ is measured first, and the observable B corresponding to a POVM $\hat{F}(b)$ is measured second, the joint probability density is

$$P(a, b) = Tr \left(\hat{\rho}_0 \sqrt{\hat{E}}(a) \hat{F}(b) \sqrt{\hat{E}}(a) \right), \quad (82)$$

where $\hat{\rho}_0$ is the initial state. Eq. (81) cannot be brought in the form (82). This is not surprising since the two measurements in Eq. (82) take place at fixed time instants, while time is a random variable in time-of-arrival measurements.

5.2 Marginal distributions

The two marginal distributions of the probability density(81) have different properties. When tracing out the time t_2 of the second measurement, we recover the probability distribution $P^{(1)}_{id}(L_1, t_1)$ of Eq. (19),

$$\int_{-\infty}^{\infty} dt_2 P^{(2)}_{id}(L_1, t_1; L_2, t_2) = P^{(1)}_{id}(L_1, t_1). \quad (83)$$

By causality, the second measurement cannot affect the statistics of the first one.

However, when tracing out the time t_1 of the first measurement, we obtain a probability distribution that differs from $P^{(1)}_{id}(L_2, t_2)$,

$$\int_{-\infty}^{\infty} dt_1 P^{(2)}_{id}(L_1, t_1; L_2, t_2) = \int \frac{dk dk'}{2\pi} \frac{\sqrt{m}(\epsilon_k + \epsilon_{k'})^{3/2}}{|kk'|} e^{i(k - k')L_2 - i(\epsilon_k - \epsilon_{k'})t_2} \tilde{\psi}^*_0(k') \tilde{\psi}_0(k). \quad (84)$$

The marginal distribution (84) is of the form (41) for

$$\eta(x) = \frac{(1 + \frac{x^2}{16})^{3/2}}{1 - \frac{x^2}{16}}. \quad (85)$$

Eq. (84) implies that the first measurement has transformed the initial state $\hat{\rho}_0$ as

$$\hat{\rho}_0 \to \left(\hat{p} \hat{\rho}_0 \hat{p}^{-1} + \hat{p}^{-1} \hat{\rho}_0 \hat{p} \right). \quad (86)$$

In order to find the analogue of the state reduction for a time-of-arrival measurement, we write Eq. (81) as

$$P^{(2)}_{id}(L_1,t_1;L_2,t_2)=\int\frac{dkdk'}{2\pi}\sqrt{\frac{\epsilon_k+\epsilon_{k'}}{m}}e^{i(k-k')(L_2-L_1)-i(\epsilon_k-\epsilon_{k'})(t_2-t_1)}\rho^{(red)}_{L_1,t_1}(k,k'), \tag{87}$$

where

$$\begin{aligned}\rho^{(red)}_{L,t}(k,k')&=\frac{\epsilon_k+\epsilon'_k}{m}\int\frac{dk_1dk'_1}{\pi}\delta(\epsilon_k+\epsilon_{k'}-\epsilon_{k_1}-\epsilon_{k'_1})e^{i(k_1-k'_1)L-i(\epsilon_{k_1}-\epsilon_{k'_1})t}\rho_0(k,k')\\&=\frac{\epsilon_k+\epsilon_{k'}}{\pi m}\int_{-\infty}^{\infty}dse^{is(\epsilon_k+\epsilon_{k'})}\langle L|e^{i\hat{H}(t+s)}\hat{\rho}_0e^{-i\hat{H}(t-s)}|L\rangle\end{aligned} \tag{88}$$

Thus, a measurement by a detector at L that records the value t changes the state of the system, by a generalized 'state reduction' rule

$$\hat{\rho}_0\to\hat{\rho}^{(red)}_{L,t}=\frac{1}{\pi m}\int_{-\infty}^{\infty}ds\langle L|e^{i\hat{H}(t+s)}\hat{\rho}_0e^{-i\hat{H}(t-s)}|L\rangle\left[\hat{H}|s\rangle\langle -s|+|s\rangle\langle -s|\hat{H}\right], \tag{89}$$

where $|s\rangle=\int_0^\infty dke^{is\epsilon_k}|k\rangle$.

Obviously, the rule (89) is very different from the standard rule of quantum state reduction. This is not surprising, because a time-of-arrival measurement refers to a fixed point in space and variable time, in contrast to the usual reduction rule that refers to a fixed instant of time. We note that the transformation (89) is constructed solely from the Hamiltonian $\hat{H}$ and the generalized eigenstates of the position operator.

5.3 Classical correspondence

We rewrite Eq. (81) as

$$P^{(2)}_{id}(L_1,t_1;L_2,t_2)=\int dkdk'\psi_0^*(k')\psi_0(k)\langle k|\hat{\Pi}_{L_1}(t_1)|k'\rangle F(\epsilon_k+\epsilon_{k'},L_2-L_1,t_2-t_1), \tag{90}$$

where $\langle k|\hat{\Pi}_{L_1}(t)|k'\rangle$ is given by Eq. (20) and

$$F(E,\ell,\tau)=\frac{2E}{\pi m}\int_0^\infty dk\int_0^\infty dk'e^{i(k-k')\ell-i(\epsilon_k-\epsilon_{k'})\tau}\delta(\epsilon_k+\epsilon_{k'}-E). \tag{91}$$

The Fourier transform of the function F with respect to τ is readily evaluated,

$$\tilde{F}(E,\ell,\mu):=\begin{cases}\int d\tau e^{-i\mu\tau}F(\epsilon,\ell,\tau)=\frac{E}{\sqrt{E^2-\mu^2}}e^{i\sqrt{m(E-\mu)}\ell-\sqrt{m(E+\mu)}\ell}, & \mu\le E\\ 0 & \mu>E\end{cases}. \tag{92}$$

In the Appendix B.2, we obtain an analytic expression for the function F, using a stationary phase approximation to the inverse Fourier transform of $\tilde{F}$. Here, we note that

for $|\mu| << E$, $\tilde{F}(E,\ell,\mu) \simeq e^{-i\sqrt{m/E}\ell\mu}$. Hence, for sufficiently large times ($E\tau >> 1$), F approximates a delta function,

$$F(E,\ell,\tau) \simeq \delta(\tau - \sqrt{\frac{m}{E}}\ell). \tag{93}$$

Transforming Eq. (90) into the Wigner picture, we obtain

$$P^{(2)}_{id}(L_1,t_1;L_2,t_2) = \int dXdPW_0(X,P)$$
$$\times \left(\frac{1}{2\pi m} \int d\xi e^{i\xi(L_1 - X - \frac{P}{m}t_1)} \sqrt{P^2 + \frac{\xi^2}{4}} F(\frac{P^2}{m} + \frac{\xi^2}{4m}, L_2 - L_1, t_2 - t_1) \right). \tag{94}$$

An inspection of Eq. (24) shows that the classical time-of-arrival probability distribution corresponds to the limit $|\xi| << |P|$ in the integral. This is the same regime in which Eq. (93) applies. Approximating $P^2 + \xi^2/4 \simeq P^2$ and using Eq. (93), we obtain the classical probability distribution for two successive time-of-arrival measurements

$$P^{(2)}_{cl}(L_1,t_1;L_2,t_2) = \int dXdP\ W_0(X,P)\delta(t_1 - T_{c1})\delta(t_2 - t_1 - T_{c2} + T_{c1}), \tag{95}$$

where

$$T_{ci} = m\frac{L_i - X}{P}. \tag{96}$$

5.4 Time-of-flight velocity

Next, we define the probability density $P(\tau)$ for the *time-of-flight* $\tau = t_2 - t_1$ between the two measurements

$$P(\tau) := \int dt P^{(2)}_{id}(L_1,t;L_2,t+\tau) = \int dk |\tilde{\psi}_0(k)|^2 F(2\epsilon_k, L_2 - L_1, \tau). \tag{97}$$

We use the term 'time of flight' as distinct from the term 'time of arrival'. The time of arrival refers to one measurement record on a single detector, while the time of flight requires two measurement records at spatially separated detectors.

The time of flight τ and the time t_1 of the first measurement are uncorrelated: the correlation function $C_{t_1\tau}$, calculated from Eq. (90), vanishes.

Eq. (97) implies that the time of flight can be represented by an operator $\hat{\tau}$ that is a function of the momentum $\hat{p}$: $\hat{\tau} = \tau_f(|\hat{p}|)$, where

$$\tau_f(p) = \int_0^\infty dss F(\frac{p^2}{m}, L_2 - L_1, s). \tag{98}$$

We also define the *time-of-flight velocity*

$$v_{tof}(p) := \frac{L_2 - L_1}{\tau_f(p)}. \tag{99}$$

In the regime where Eq. (93) applies, Eq. (98) yields $\tau_f(p) = m(L_2 - L_1)/p$. Hence,

$$v_{tof}(p) = \frac{p}{m}, \tag{100}$$

i.e., the time-of-flight velocity coincides with the canonical velocity p/m. This result agrees with the classic analysis of Park and Margenau [32], even though the context is slightly different. The difference is that the time-of-flight velocity is defined here in terms of two measurements of time at specific locations, while in Park and Margenau's work, the time-of-flight velocity is defined in terms of two position measurements at pre-specified times.

In general, probabilities associated to velocity differ from the probabilities associated to momentum. This is because momentum and velocity are defined differently in any histories-based theory [11]. This difference is manifested in temporally extended measurements. For example, in time-extended von Neumann measurements, velocity and momentum correspond to different Hamiltonian operators for the interaction between the quantum system and the measurement apparatus [33].

This difference turns out to be insignificant for time-of-flight velocities. The evaluation of (99) using the approximation (122) of the Appendix B.2 yields appreciable differences from Eq. (100) only for $(L_2 - L_1)p << 1$, i.e., when the distance between the detectors is *much smaller* than the de Broglie wavelength of the particles.

6 Conclusions

The main result of this paper is the construction of time-of-arrival probabilities for multi-partite systems and for sequential measurements. This was made possible by the use of the QTP method, in which the relevant probabilities are constructed as linear functionals of appropriate field correlation functions. The method can be straightforwardly generalized to set-ups more elaborate than the ones considered here, involving three or more detection events.

When the time-of-arrival problem is formulated in terms of a single particle and a single detector, all approaches lead to almost indistinguishable predictions. In multi-partite systems, this is no longer the case. Approaches to the time of arrival based on probability currents lead to quantitatively different predictions from those based on POVMs. Therefore, we propose that measurements of time-of-arrival correlations in multi-partite systems can distinguish between different theories about the time of arrival.

Besides the main result above, we also showed that the time-of-arrival correlations can play the role of entanglement witness in multi-partite systems. This result suggests that temporal observables can be used for the retrieval of quantum information and might even be employed in quantum information processing. We also derived the probability distribution associated to sequential time-of-arrival measurements, and we found that the state-reduction rule for a time-of-arrival measurement is very different from the standard one.

References

[1] J. C. Muga and J. R. Leavens, *Arrival time in quantum mechanics*, Phys. Rep. 338, 353 (2000).

[2] J. C. Muga, R. S. Mayato, and I. L. Equisquiza, *Time in Quantum Mechanics, vol 1* (Springer 2008); J. G. Muga, A Ruschhaupt and A. Del Campo, *Time in Quantum Mechanics, vol 2* (Springer 2010).

[3] W. Pauli, *The Principles of Quantum Mechanics*, in *Encyclopedia of Physics*, edited by S. Flugge, Vol. 5/1 (Springer, Berlin, 1958).

[4] C. Anastopoulos and N. Savvidou, *Time-of-arrival Probabilities for General Particle Detectors*, Phys. Rev. A86, 012111 (2012).

[5] C. Anastopoulos and N. Savvidou, *Quantum temporal probabilities in tunneling systems*, Ann. Phys. 336, 281 (2013).

[6] C. Anastopoulos and N. Savvidou, *Time-of-arrival Probabilities and Quantum Measurements*, J. Math. Phys. 47, 122106 (2006).

[7] C. Anastopoulos and N. Savvidou, *Time-of-arrival probabilities and quantum measurements. II. Application to tunneling times*, J. Math. Phys. 49, 022101 (2008).

[8] C. Anastopoulos, *Time-of-arrival probabilities and quantum measurements. III. Decay of unstable states*, J. Math. Phys. 49, 022103 (2008).

[9] C. Anastopoulos and N. Savvidou, *Coherences of Accelerated Detectors and the Local Character of the Unruh Effect*, J. Math. Phys. 53, 012107 (2012); *Real-time particle-detection probabilities in accelerated macroscopic detectors*, Gen. Rel. Grav. 47, 1842 (2015).

[10] C. Anastopoulos and N. Savvidou, *Measurements on relativistic quantum fields: I. Probability assignment* arXiv:1509.01837; *Measurements on relativistic quantum fields: II. Detector Models*, arXiv:1509.01838.

[11] K. Savvidou, *The Action Operator for Continuous-time Histories* J. Math. Phys. 40, 5657 (1999); *Continuous Time in Consistent Histories*, gr-qc/9912076.

[12] N. Savvidou, *Space-time Symmetries in Histories Canonical Gravity*, in "Approaches to Quantum Gravity", edited by D. Oriti (Cambridge University Press, Cambridge 2009).

[13] M. Gell-Mann and J. B. Hartle, *Quantum Mechanics in the Light of Quantum Cosmology*, in 'Complexity, Entropy, and the Physics of Information', ed. by W. Zurek, (Addison Wesley, Reading 1990); *Classical Equations for Quantum Systems*, Phys. Rev. D47, 3345 (1993).

[14] J. Kijowski, *On the time operator in quantum mechanics and the Heisenberg uncertainty relation for energy and time*, Rep. Math. Phys. 6, 361 (1974).

[15] R. F. Werner, *Wigner quantisation of arrival time and oscillator phase*, J. Phys. A: Math. Gen. 21, 4565 (1988).

[16] Y. Aharonov and D. Bohm, *Time in the Quantum Theory and the Uncertainty Relation for Time and Energy*, Phys. Rev. 122, 1649 (1961).

[17] A. D Baute, R. Sala Mayato, J. P. Palao, J. G. Muga, and I. L. Egusquiza, *Time-of-arrival distribution for arbitrary potentials and Wigner's time-energy uncertainty relation*, Phys. Rev. A61, 022118 (2000).

[18] Y. Aharonov, J. Oppenheim, S. Popescu, B. Reznik, and W. G. Unruh, *Measurement of Time-of-Arrival in Quantum Mechanics*, Phys. Rev. A57, 4130 (1998).

[19] J. Echanobe, A. del Campo, and J. G. Muga, *Disclosing hidden information in the quantum Zeno effect: Pulsed measurement of the quantum time of arrival*, Phys. Rev. A, 77, 032112 (2008),

[20] J. J. Halliwell and J. M. Yearsley, *Arrival Times, Complex Potentials and Decoherent Histories*, Phys. Rev. A79, 062101 (2009).

[21] J. M. Yearsley, D. A. Downs, J. J. Halliwell, and A. K. Hashagen, *Quantum Arrival and Dwell Times via Idealised Clocks*, Phys. Rev. A 84, 022109 (2011).

[22] V. Delgado and J. G. Muga, *Arrival time in quantum mechanics*, Phys. Rev. A56, 3425 (1997).

[23] R. de la Madrid and J. Isidro, *The HFT Selfadjoint Variant of Time Operators*, Adv. Stud. Theor. Phys. 2, 281 (2008).

[24] A. D. Baute, I. L. Egusquiza, J. G. Muga and R. Sala-Mayato, *Time-of-arrival distributions from position-momentum and energy-time joint measurements*, Phys. Rev. A61, 052111 (2000).

[25] J. A. Damborenea, I. L. Egusquiza, G. C. Hegerfeldt, J. G. Muga, *A measurement-based approach to quantum arrival times*, Phys. Rev. A 65, 052104 (2002).

[26] J. J. Halliwell, J. Evaeus, J. London, and Y. Malik, *A self-adjoint arrival time operator inspired by measurement models*, Phys. Lett. A379, 2445 (2015).

[27] G. R. Allcock, *The time of arrival in quantum mechanics I. Formal considerations*, Ann.Phys 53, 253 (1969); *The time of arrival in quantum mechanics II. The individual measurement*, Ann. Phys. 53, 286 (1969); *The time of arrival in quantum mechanics III. The measurement ensemble*, Ann. Phys. 53, 311 (1969).

[28] A. J. Bracken and G. F. Melloy, *Probability backflow and a new dimensionless quantum number*, Phys. A27, 2197 (1994).

[29] D. F. Walls and G. J. Milburn, *Quantum Optics* (Springer, 2008).

[30] A. Peres, *Separability Criterion for Density Matrices*, Phys. Rev. Lett. 77, 1413 (1996); M. Horodecki, P. Horodecki and R. Horodecki, *Separability of Mixed States: Necessary and Sufficient Conditions*, Phys. Lett. A223, 1 (1996).

[31] R. Simon, *Peres-Horodecki separability criterion for continuous variable systems*, Phys. Rev. Lett. 84, 2726 (2000).

[32] J. L. Park and H. Margenau, *Simultaneous Measurability in Quantum Theory*, Int. J. Theor. Phys. 1, 211 (1968).

[33] C. Anastopoulos and N. Savvidou, *Quantum probabilities for time-extended alternatives*, J. Math. Phys. 48, 032106 (2007).

[34] J.B. Hartle, *Spacetime Quantum Mechanics and the Quantum Mechanics of Spacetime* in 'Gravitation and Quantizations', in the Proceedings of the 1992 Les Houches Summer School , ed. by B. Julia and J. Zinn- Justin, Les Houches Summer School Proceedings, Vol. LVII, (North Holland, Amsterdam, 1995); [gr-qc/9304006].

A The Quantum Temporal Probabilities method

A.1 General probability assignment

We consider a composite physical system that consists of a microscopic and a macroscopic component. The microscopic component is the quantum system to be measured and the macroscopic component is the measuring device.

We denote the Hilbert space associated to the composite system by $\mathcal{H}$. We describe a measurement event as a transition between two complementary subspaces of $\mathcal{H}$. To this end, we split $\mathcal{H}$ in two subspaces: $\mathcal{H} = \mathcal{H}_+ \oplus \mathcal{H}_-$. The subspace $\mathcal{H}_+$ describes the accessible states of the system given that the event under consideration is realized. For example, if the event is a detection of a microscopic particle by an apparatus, $\mathcal{H}_+$ corresponds to all states of the apparatus compatible with the macroscopic record of detection. We denote the projection operator onto $\mathcal{H}_+$ as $\hat{P}$ and the projector onto $\mathcal{H}_-$ as $\hat{Q} := 1 - \hat{P}$. We assume that the system is described by a Hamiltonian operator $\hat{H}$.

In Refs. [4, 10], we constructed the probability density with respect to time that is associated to the transition of the system from $\mathcal{H}_-$ to $\mathcal{H}_+$. A pointer variable λ of the measurement apparatus was also assumed to take a definite value after the transition has occurred. It is described by a set of positive operators $\hat{\Pi}(\lambda)$ that correspond to the different values of λ. The operators $\hat{\Pi}(\lambda)$ satisfy $\sum_\lambda \hat{\Pi}(\lambda) = \hat{P}$.

First, we construct the probability amplitude $|\psi; \lambda, [t_1, t_2]\rangle$ that, given an initial ($t = 0$) state $|\psi_0\rangle \in \mathcal{H}_-$, a transition occurs during the time interval $[t_1, t_2]$ and a value λ for the pointer variable is obtained for some observable. For a vanishingly small time interval, i.e., $t_1 = t$ and $t_2 = t + \delta t$, one obtains [4]

$$|\psi_0; \lambda, [t, t + \delta t]\rangle = -i\, \delta t\; e^{-i\hat{H}(T-t)} \sqrt{\hat{\Pi}}(\lambda) \hat{H} \hat{S}_t |\psi_0\rangle, \tag{101}$$

where $\hat{S}_t = \lim_{N\to\infty} (\hat{Q} e^{-i\hat{H}t/N} \hat{Q})^N$ is the restricted propagator in the subspace $\mathcal{H}_-$.

The amplitude (101) defines a *density* with respect to time: $|\psi_0; \lambda, t\rangle = -ie^{-i\hat{H}T} \hat{C}(\lambda, t)|\psi_0\rangle$, where $\hat{C}(\lambda, t) := e^{i\hat{H}t} \sqrt{\hat{\Pi}}(\lambda) \hat{H} \hat{S}_t$ is a *history operator*. The total amplitude that the transition occurred at *some moment* within a time interval $[t_1, t_2]$ is

$$|\psi; \lambda, [t_1, t_2]\rangle = -ie^{-i\hat{H}T} \int_{t_1}^{t_2} dt \hat{C}(\lambda, t)|\psi_0\rangle. \tag{102}$$

Eq. (102) involves the restricted propagator $\hat{S}_t$ which may be difficult to evaluate in practice. We sidestep the evaluation of $\hat{S}_t$, by using the following approximation. We consider a Hamiltonian $\hat{H} = \hat{H}_0 + \hat{H}_I$ where $[\hat{H}_0, \hat{P}] = 0$, and H_I is a perturbing interaction. To leading order in the interaction,

$$\hat{C}(\lambda, t) = e^{i\hat{H}_0 t} \sqrt{\hat{\Pi}}(\lambda) \hat{H}_I e^{-i\hat{H}_0 t}, \tag{103}$$

with no dependence on $\hat{S}_t$. All models for relativistic measurements we consider in this paper use the approximation (103).

We construct a probability measure from the amplitude (102) by coarse-graining the time variable [4, 10]. This is a natural procedure for systems that involves a macroscopic component such as a measuring apparatus [13, 34]. Hence, probabilities are defined only for time intervals $]t_1, t_2]$ such that $|t_2 - t_1| >> \sigma$, where σ is the coarse-graining scale.

We implement temporal coarse-graining by defining smeared history operators, $\hat{C}_f(\lambda, t) = \int ds \sqrt{f}(t-s)\hat{C}(\lambda, s)$. The function $f(s)$ is positive, it is centered around $s = 0$ and has width of order σ, like, for example, the Gaussian (5). The probability density that a transition occurs during the time interval $[t_1, t_2]$ and a value λ for the pointer variable is obtained is

$$P(\lambda, t) = Tr[\hat{C}_f(\lambda, t)\hat{\rho}_0\hat{C}_f^\dagger(\lambda, t)], \tag{104}$$

where $\hat{\rho}_0 = |\psi_0\rangle\langle\psi_0|$.

An analogous equation holds for multiple events. The probability density that one event associated to a measurement record λ_1 occurs at time t_1, and another event associated to a measurement record $\lambda_2$occurs at time t_2 is

$$P(\lambda_1, t_1; \lambda_2, t_2) = Tr\left[\hat{C}_{f_1,f_2}(\lambda_1, t_1, \lambda_2, t_2)\hat{\rho}_0\hat{C}_{f_1,f_2}(\lambda_1, t_1, \lambda_2, t_2)\right], \tag{105}$$

where

$$\hat{C}_{f_1,f_2}(\lambda_1, t_1, \lambda_2, t_2) = \int ds_1 ds_2 f_1(t_1 - s_1) f_2(t_2 - s_2)\hat{C}(\lambda_1, t_1, \lambda_2, t_2) \tag{106}$$

is the smeared form of the amplitude operator

$$\hat{C}(\lambda_1, t_1, \lambda_2, t_2) = \mathcal{T}([\hat{C}_2(\lambda_2, t_2)\hat{C}_1(\lambda_1, t_1)], \tag{107}$$

where $\mathcal{T}$ is the standard time-ordering operator and $\hat{C}_i(\lambda_i, t_i)$ are the class operators (103) for a the i-th event.

A.2 Time of arrival probabilities

Next, we specialize to time of arrival measurements. In this case, the measured quantum system consists of free particles and the records of observation λ are identified with the location $\boldsymbol{L}$ of a particle detector.

Let $\mathcal{F}$ be the Hilbert space associated to the particles. For treating multi-particle states, it is convenient to identify $\mathcal{F}$ with a Fock space, either bosonic or fermionic. Hence, $\mathcal{F}$ carries either a representation of the canonical commutation relations (1), or of the canonical anti-commutation relations (2). We will denote the Hamiltonian on $\mathcal{F}$ by $\hat{h}$ and the initial state of the field by $|\Psi_0\rangle$. Ignoring spin and internal degrees of freedom, and restricting to non-relativistic particles, the field operators on $\mathcal{F}$ are defined by Eq. (3).

We assign a Hilbert space $\mathcal{K}_i$ to each detector. Thus, for a single detection event, the Hilbert space of the total system is $\mathcal{H}_1 = \mathcal{F} \otimes \mathcal{K}_1$ and for two detection events the Hilbert

space of the total system is $\mathcal{H}_2 = \mathcal{F} \otimes \mathcal{K}_1 \otimes \mathcal{K}_2$. We will denote the initial state of each detector as $|\Phi_0^{(i)}\rangle$.

We make the common assumption in von Neumann measurements that the self-dynamics of the detector is negligible. This implies that the unperturbed Hamiltonian $\hat{H}_0$ is $\hat{h} \otimes \hat{1}$ on $\mathcal{H}_1$ and $\hat{H}_0 = \hat{h} \otimes \hat{1} \otimes \hat{1}$ on $\mathcal{H}_2$. We assume a local Hamiltonian governing the interaction between the particles and the detector of the form $\hat{H}_I = \int d^3x \hat{Y}_a(\boldsymbol{x}) \otimes J^a(\boldsymbol{x})$, where $\hat{Y}_a$ are composite operators on $\mathcal{F}$ and $\hat{J}^a(\boldsymbol{x})$ are current operators on the Hilbert space of the detector.

Two cases are of particular interest.

1. An interaction Hamiltonian linear with respect to the fields

$$\hat{H}_I = \int d^3x \left[\psi(\boldsymbol{x}) \otimes \hat{J}(\boldsymbol{x}) + \hat{\psi}^\dagger(\boldsymbol{x}) \otimes \hat{J}^\dagger(\boldsymbol{x}) \right]. \tag{108}$$

   This Hamiltonian corresponds to detection by particle absorption. In order to avoid spurious signals in the detector, it is necessary to assume that the initial state $|\Phi_0\rangle$ of the apparatus satisfies $\hat{J}^\dagger|\Phi_0\rangle = 0$. Hence, $\hat{Y}$ effectively coincides with $\psi(\boldsymbol{x})$.

2. An interaction Hamiltonian $\hat{H}_I = \int d^3x \hat{\psi}^\dagger(\boldsymbol{x})\hat{\psi}(\boldsymbol{x}) \otimes \hat{J}(\boldsymbol{x})$ that is quadratic to the fields corresponds to the scattering of the detected particle. The associated composite operator $\hat{Y}(\boldsymbol{x})$ is the particle density $\hat{\psi}^\dagger(\boldsymbol{x})\hat{\psi}(\boldsymbol{x})$.

The interaction Hamiltonian of the two-detector system is

$$\hat{H}_I = \int d^3x \left(\hat{Y}_1(\boldsymbol{x}) \otimes \hat{J}_1(\boldsymbol{x}) \otimes \hat{1} + \hat{Y}_2(\boldsymbol{x}) \otimes \hat{1} \otimes \hat{J}_2(\boldsymbol{x}) \right). \tag{109}$$

The detectors are assumed to be static and localized in position. Thus, a detection event corresponds to a position pointer variable $\boldsymbol{L}$, described by positive operators $\hat{P}_{\boldsymbol{L}}$ on the Hilbert space $\mathcal{K}$ of the detector. This implies that the positive operator $\hat{\Pi}_\lambda$ in Eq. (103) is $\hat{1} \otimes \hat{P}_{\boldsymbol{L}}$ on $\mathcal{H}_2$.

Assuming an initial state $|\Psi_0\rangle \in \mathcal{F}$ for the particles and an initial state $|\Phi_0\rangle \in \mathcal{K}_1$ for the detector, Eq. (103) yields

$$P(\boldsymbol{L}, t) = \int ds ds' \sqrt{f(t-s)f(t-s')} \int d^3x d^3x' \langle \Psi_0 | Y^\dagger(\boldsymbol{x}', s') \hat{Y}(\boldsymbol{x}, s) | \Psi_0 \rangle \times \langle \Phi_0 | \hat{J}^\dagger(\boldsymbol{x}') \hat{P}_{\boldsymbol{L}} \hat{J}(\boldsymbol{x}) | \Phi_0 \rangle. \tag{110}$$

If the distance between the particle source from the detector is much larger than the size of the detector, $\hat{P}_{\boldsymbol{L}} \hat{J}(\boldsymbol{x})|\Phi_0\rangle$ vanishes unless $\boldsymbol{L} \simeq \boldsymbol{x}$. Ignoring position coarse-graining, we can approximate

$$\langle \Phi_0 | \hat{J}^\dagger(\boldsymbol{x}') \hat{P}_{\boldsymbol{L}} \hat{J}(\boldsymbol{x}) | \Phi_0 \rangle = C \delta^3(\boldsymbol{x} - \boldsymbol{L}) \delta^3(\boldsymbol{x} - \boldsymbol{L}), \tag{111}$$

for some positive constant C. Hence, Eq. (110) gives Eq. (4).

Using the same procedure, one obtains Eq. (10) from Eq. (105).

B Functions that appear in probability distributions

B.1 The distribution $u(s)$, Eq. (25)

The integral $u(s)$, Eq. (25), defines a probability distribution that is singular at $s = 0$, and it is characterized by a moment-generating functional

$$z(\mu) := \int ds u(s) e^{i\mu s} = \sqrt{1+\mu^2} \tag{112}$$

The moments of $u(s)$ are obtained from the differentiation of $Z(\mu)$ at $\mu = 0$,

$$\int ds s^n u(s) = \begin{cases} \frac{1}{2^k} & n = 2k, k = 0, 1, 2. \\ \frac{1\cdot 3\cdot \ldots \cdot (2k-3)}{2^k} & n = 2k, k = 3, 4, \ldots \\ 0 & n = 2k+1, k = 0, 1, 2, \ldots . \end{cases} \tag{113}$$

The distribution $u(s)$ is best characterized as

$$u(s) = \frac{d}{ds}\zeta(s) \tag{114}$$

where $\zeta(s)$ is the weak limit of the family of functions

$$\zeta_\epsilon(s) = \frac{1}{\pi}\int_0^\infty dk \frac{\sin ks}{k}\sqrt{1+k^2}e^{-k\epsilon}, \tag{115}$$

as $\epsilon \to 0$.

For large values of $|s|$, the dominant contribution to the integral (115) is

$$\frac{1}{\pi}\int_0^\infty dk \frac{\sin ks}{k},$$

which has a finite value $\frac{1}{2}\mathrm{sgn}(s)$. Hence $\zeta(s) \simeq \theta(s) - \frac{1}{2}$, where $\theta(s)$ is the Heavyside step function. This approximation that justifies the substitution of $u(s)$ with a delta function, since $\delta(s) = \frac{d}{ds}\theta(s)$.

For s around zero,

$$\zeta_\epsilon(s) \simeq \frac{1}{\pi}\int_0^\infty dk \sin ks e^{-k\epsilon} = \frac{1}{\pi}\frac{s}{s^2+\epsilon^2}. \tag{116}$$

Eq. (116) implies that in the vicinity of $s = 0$, ζ approaches the distribution $\mathrm{PV}\frac{1}{s}$, where PV stands for the Cauchy principal value.

The distribution $\zeta(s)$ decreases everywhere with s except for the infinite jump from $-\infty$ to ∞ at $s = 0$. Even if $u(s) < 0$ everywhere but $s = 0$, the positive contribution from the infinite jump dominates over the negative values so that the moments (113) turn out to be positive. However, the integral $\int_{-\infty}^\infty ds u(s) f(s)$ is negative for any smooth positive function $f(s)$ that vanishes in an open neighborhood of $s = 0$.

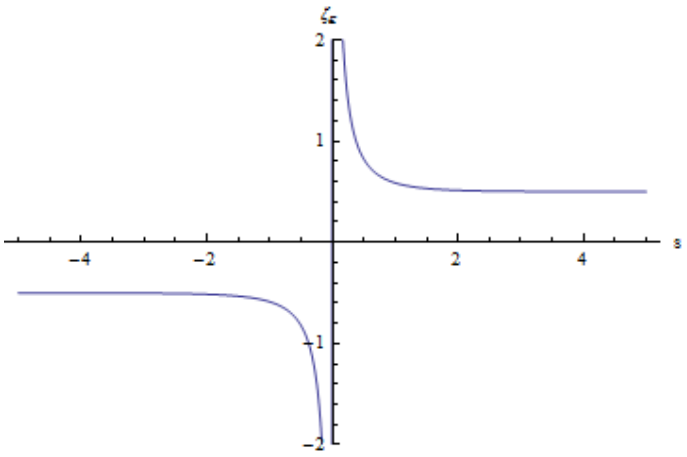

Figure 4: Graph of the function $\zeta_\epsilon(s)$ of Eq. (115) for $\epsilon = 10^{-5}$.

Regarding the role of $u(s)$ in the probability density (24), we note the following. If Eq. (24) involved a classical probability distribution rather than a Wigner function, the probabilities Eq.(24) could become negative. A classical probability distribution can have support on a bounded region U of the (X, P) plane, so that the argument of u in Eq. (24) cannot becomes zero for $(X, P) \in U$. However, unlike a classical probability distribution, a Wigner function cannot be sharply localized in a bounded region. Since the argument of u in Eq. (24) involves both X and P, it will always cross $s = 0$, even if $s = 0$ corresponds to a tail of the Wigner function. Hence, the densities (24) are positive for Wigner functions, but they can be negative for classical probability distributions that are not Wigner functions of some quantum state.

B.2 The function $F(E, \ell, \tau)$, Eq. (91)

We compute $F(E, \ell, \tau)$ by evaluating the inverse Fourier transform of Eq. (92). Setting $x = \mu/E$, we find

$$F(E, \ell, \tau) = \frac{E}{2\pi} \int_{-1}^{1} \frac{dx}{\sqrt{1 - x^2}} e^{i(E\tau)S(x)}, \tag{117}$$

where

$$S(x) = x - \gamma(\sqrt{1 + x} - \sqrt{1 - x}), \tag{118}$$

for

$$\gamma = \sqrt{\frac{m}{E}} \frac{\ell}{\tau}. \tag{119}$$

For $\gamma < 1$, the function $S(x)$ has two critical points at $x = \pm x_0$, where

$$x_0 = \sqrt{1 - \frac{\gamma^2}{4}(1 + \sqrt{1 + 8/\gamma^2})}. \tag{120}$$

For $\gamma > 1$, there are no critical points.

We evaluate the integral in Eq. (117), using the stationary phase method, to obtain

$$F(E,\ell,\tau) = \sqrt{\frac{2E}{\pi B(\gamma)\tau}}\cos[A(\gamma)E\tau - \frac{\pi}{4}], \tag{121}$$

for $\gamma \leq 1$. We used the notation $A(\gamma) = S(x_0)$ and $B(\gamma) = |S''(x_0)|(1-x_0^2)$. For $\gamma > 1$, F is strongly suppressed. Within the domain of validity if Eq. (121), we can set $F(E,\ell,\tau) = 0$.

For γ close to 1, $x_0 \simeq \sqrt{\frac{4}{3}(1-\gamma)}$, and $B(\gamma) \simeq \sqrt{\frac{3}{4}(1-\gamma)}$. Hence, $F(E,\ell,\tau)$ is sharply peaked at $\gamma = 1$. When evaluating integrals of the form $\int_0^\infty d\tau F(E,\ell,\tau)g(\tau)$ for some positive function τ, only values of γ close to unity contribute significantly. In this case, the critical points of $S(x)$ are close to zero, so we are justified in expanding $S(x)$ around $x = 0$. The lowest order in the expansion leads to the classical limit, Eq. (93). Keeping terms up to the next order, we approximate

$$F(E,\ell,\tau) \simeq \frac{E}{2\pi}\int_{-\infty}^{\infty} dx e^{iE\tau[x-\gamma(x+\frac{1}{8}x^3)]} = D\ \mathrm{Ai}[-D(\tau - \sqrt{m/E}\ell)], \tag{122}$$

where Ai is the Airy function and $D = 2\left(\frac{E^5}{9m\ell^2}\right)^{1/6}$.